Elsevier Editorial System(tm) for Journal of Hydrology

Manuscript Draft

Manuscript Number:

Title: Non-Fickian dispersive transport of strontium in laboratory-scale columns:Modelling and evaluation

Article Type: Research Paper

Keywords: Non-Fickian transport; Dispersion; CTRW; Preferential flow; Sorption

Corresponding Author: Mr. Dongxu Liu,

Corresponding Author's Institution: Northwest Institute of Nuclear Technology

First Author: Dongxu Liu

Order of Authors: Dongxu Liu; Andrey P Jivkov; Lichun Wang; Gaohua Si; Jing Yu

Abstract: In the context of environmental remediation of contaminated sites and safety assessment of nuclear waste disposal in the near-surface zone, we investigate the leaching and non-Fickian dispersive migration with sorption of strontium (mocking strontium-90) through columns packed with sand and clay. Analysis is based on breakthrough curves (BTCs) from column experiments, which simulated rainfall infiltration and source term release scenario, rather than applying constant tracer solution at the inlet as commonly used. BTCs are re-evaluated and transport parameters are estimated by inverse modelling using two approaches: (1) equilibrium advection-dispersion equation (ADE); and (2) continuous time random walk (CTRW). Firstly, based on a method for calculating leach concentration, the inlet condition with an exponential decay input is identified. Secondly, the results show that approximately 39%~58% of bromine and 16%~49% of strontium are eluted from the columns at the end of the breakthrough experiments. This suggests that trapping mechanisms, including diffusion into immobile zones and attachment of tracer on mineral surfaces, are more pronounced for strontium than for bromine. Thirdly, we demonstrate robustness of CTRW-based truncated power-law (TPL) model in capturing non-Fickian reactive transport with $0<\beta<2$, and Fickian transport with $\beta>2$. The non-Fickian dispersion observed experimentally is explained by variations of local flow field from preferential flow paths due to physical heterogeneities. Particularly, the additional sorption process of strontium on clay minerals contributes to the delay of the peak concentration and the tailing features, which leads to enhanced non-Fickian transport for strontium. Finally, the ADE and CTRW approaches to environmental modelling are evaluated. It is shown that CTRW with a sorption term can describe non-Fickian dispersive transport of strontium at laboratory scale by identifying appropriate parameters, while the traditional ADE with a retardation factor fails to reproduce the complex non-Fickian transport of strontium with remarkable sorption on clay surface.

Suggested Reviewers: Diogo Bolster PhD

Assistant Professor, Civil & Environmental Engineering and Earth Sciences, University of Notre Dame
bolster@nd.edu
Dr. Diogo Bolster is an expert in flow & transport in heterogeneous porous media, particle tracking simulations for reactive transport.

Hongbin Zhan PhD
Endowed Ray C. Fish Professor in Geology, Department of Geology & Geophysics, Texas A&M University
zhan@geos.tamu.edu
Dr. Hongbin Zhan is an expert in non-Darcian flow and non-Fickian dispersion of solute transport, groundwater flow and solute transport in subsurface systems.

Scott D Hansen PhD
Postdoctoral Research Associate, Los Alamos National Laboratory
skh3@lanl.gov
Dr. Scott D. Hansen is an expert in applied mathematics and contaminant hydrogeology, include anomalous transport, random walks methods (including CTRW), and reactive transport.

Aaron Packman PhD
Associate Professor , Department of Civil and Environmental Engineering , Northwestern University
a-packman@northwestern.edu
Dr. Aaron Packman is an expert in
Environmental fluid dynamics and solute transport, including both hydrodynamic transport processes and reactive transport processes.

Yong Zhang PhD
Associate Professor, Department of Geological Sciences, The University of Alabama
yzhang264@ua.edu
Dr. Yong Zhang is an expert in Darcy-scale non-Fickian transport, numerical modeling of flow and transport in porous and fractured media.

DearEditor,

Please, consider the attached manuscript "*Non-Fickian dispersive transport of strontium in laboratory-scale columns:Modelling and evaluation*"for publication in the Journal of Hydrology.

It contains original research that has not been publishedelsewhere.We propose the integration of non-Fickian transport modelling andlaboratory dynamic column experiments mocking rainfall infiltration scenarios, and analyzenon-Fickiandispersive transportfor strontiumdue to variation of flow fields and sorption retardation processes, which is significativetoadvance the understanding and prediction of radionuclide transport through hydrologic paths and heterogeneous systems.

We believe that the methodology and the findings of this work will be of interest to the readership of your Journal.

Respectfully yours,

DongxuLiu
Andrey PJivkov
Lichun Wang
Gaohua Si
Jing Yu

- Integrated methodology for coupling release and transport of strontium
- Experimental data with Fickian and non-Fickian transport re-evaluated
- Advection-DispersionEquation and Continuous Time Random Walk examined
- ADE suitable for Fickian transport only; CTRWcapturesboth regimes
- Effects of chemical and physical heterogeneities on transport analysed

Non-Fickian dispersive transport of strontium in laboratory-scale columns: Modelling and evaluation

Dongxu Liu[1,2,*], Andrey P Jivkov[2,*], Lichun Wang[3] , Gaohua Si[1], Jing Yu[1]

[1]Northwest Institute of Nuclear Technology, Xi'an 710024, PR China

[2]Research Centre for Radwaste & Decommissioning and Modelling & Simulation Centre, Dalton Nuclear Institute, The University of Manchester, Manchester M13 9PL, UK

[3]Department of Geological Sciences, University of Texas at Austin, Austin, Texas, USA

Abstract

In the context of environmental remediation of contaminated sites and safety assessment of nuclear waste disposal in the near-surface zone, we investigate the leaching and non-Fickian dispersive migration with sorption of strontium (mocking strontium-90) through columns packed with sand and clay. Analysis is based on breakthrough curves (BTCs) from column experiments, which simulated rainfall infiltration and source term release scenario, rather than applying constant tracer solution at the inlet as commonly used. BTCs are re-evaluated and transport parameters are estimated by inverse modelling using two approaches: (1) equilibrium advection-dispersion equation (ADE); and (2) continuous time random walk (CTRW). Firstly, based on a method for calculating leach concentration, the inlet condition with an exponential decay input is identified. Secondly, the results show that approximately 39%~58% of bromine and 16%~49% of strontium are eluted from the columns at the end of the breakthrough experiments. This suggests that trapping mechanisms, including diffusion into immobile zones and attachment of tracer on mineral surfaces, are more

* Corresponding Author. E-mail: dongxu.liu@manchester.ac.uk; Andrey.Jivkov@manchester.ac.uk
Phone: +44(0)1613063765

pronounced for strontium than for bromine. Thirdly, we demonstrate robustness of CTRW-based truncated power-law (TPL) model in capturing non-Fickian reactive transport with $0<\beta<2$, and Fickian transport with $\beta>2$. The non-Fickian dispersion observed experimentally is explained by variations of local flow field from preferential flow paths due to physical heterogeneities. Particularly, the additional sorption process of strontium on clay minerals contributes to the delay of the peak concentration and the tailing features, which leads to enhanced non-Fickian transport for strontium. Finally, the ADE and CTRW approaches to environmental modelling are evaluated. It is shown that CTRW with a sorption term can describe non-Fickian dispersive transport of strontium at laboratory scale by identifying appropriate parameters, while the traditional ADE with a retardation factor fails to reproduce the complex non-Fickian transport of strontium with remarkable sorption on clay surface.

Keywords: Non-Fickian transport; Dispersion; CTRW; Preferential flow; Sorption

1. Introduction

Radioactive strontium (Sr-90), a by-product of the fission of uranium and plutonium, is found in waste from nuclear activities. Since atmospheric nuclear tests conducted in the 1950s and 1960s and the accident occurred at the Chernobyl nuclear power plant, it is well known that, like many other radioactive species, large amounts of strontium-90 were produced and dispersed worldwide in fallout into the environment (EPA, 2015). Strontium-90 is considered as one of the hazardous constituents of nuclear wastes, due to its environmental mobility, radiation exposure and biologic toxicity. Specifically, strontium-90 has chemical properties similar to calcium and therefore it tends to concentrate in the bones and teeth, and can form many chemical compounds, including halides, oxides, and sulphide. This increases the risk of bone cancer, cancer of the soft tissue near the bone, and leukaemia from internal exposure (EPA, 2015). Environmental behaviour of radioactive

strontium has therefore attracted increasing attention over the last three decades, focused on understanding migration of Sr-90 and strontium isotopes through field in situ tests, laboratory experiment analysis, natural analogue studies and computer modelling. However, accurate assessment and prediction of Sr-90 transport in complex environments remains unresolved, with limited number of investigations devoted to leaching, non-Fickian migration and sorption processes (Bencala, 1984; Bruno et al., 2002; Bugai et al., 2012; Eagling et al., 2013; Hull and Schafer, 2008; Kosakowski and Smith, 2005; Maderich et al., 2014; Miller et al., 1994; Qian et al., 2009; Rumynin, 2011; Volkova, 2009; Yin et al., 2014). Combining laboratory dynamic column experiments and theoretical modelling would contribute significantly to fundamental understanding and physically realistic description of strontium transport in porous media.

Understanding species (contaminants, tracers, solutes, nuclides or particles) fate and transport in the subsurface environment is of central importance in the frame of remediation schemes for contaminated sites and nuclear waste disposal (Bijeljic et al., 2004; Levchuk et al., 2012). The problem is challenging due to perennial complexities and strong heterogeneities in geological mass. From systematic viewpoint, a persistent issue is how to explore appropriate predictive models in the absence of sufficient information on heterogeneous hydraulic-physical-chemical properties. Traditionally, species migration in geological systems from the pore scale upwards is described by Fickian-based advection-dispersion equation (ADE) models, adopting deterministic and/or stochastic approaches (Bear and Cheng, 2010; Berkowitz et al., 2001; Rumynin, 2011). However, the ADE-based approaches often fail to capture and predict non-Fickian (or anomalous) transport of species in the subsurface. This is commonly observed both in the laboratory and in the field (Berkowitz et al., 2001; Bijeljic et al., 2013; Neuman and Tartakovsky, 2009), and now recognized as ubiquitous in the transport in fractured porous media.

Non-Fickian transport behaviour presents different forms and traits, commonly referred to as scale-dependent dispersion, but manifests through "unusual" early breakthrough times and long late

time tails in measured breakthrough curves (BTCs), which deviate from the Gaussian distributions of species concentration (Bakshevskaia and Pozdniakov, 2015; Berkowitz et al., 2006; Edery et al., 2014). The continuous time random walk (CTRW) has been shown to be a successful framework to quantify non-Fickian transport with capacity to capture the transport transition from non-Fickian to Fickian (Berkowitz et al., 2006; Hansen and Berkowitz, 2015). The CTRW approach describes the random movement of solute particles in an Eulerian–Lagrangian framework (Neuman and Tartakovsky, 2009). The use of CTRW for species transport in porous and fractured media across different scales have been presented elsewhere (e.g. Berkowitz et al., 2006; Berkowitz and Scher, 2009; Blunt et al., 2013; Cortis and Berkowitz, 2004; Edery et al., 2013; Rhodes et al., 2008; Wang and Cardenas, 2014).

In the CTRW framework, the conservative tracer (e.g. bromide) parameters, including mean fluid velocity and dispersion coefficient, are inappropriate to describe transport of reactive or sorbing tracers (e.g. atrazine, TBNPA) through laboratory columns (Li and Ren, 2009; Rubin et al., 2012). Although models for describing non-Fickian transport, including mobile-immobile, fractional derivative, and multi-rate mass transport, have been applied to simulate certain pollutants transport process (e.g. pesticides), few studies focused on the application of those models to the fate of reactive nuclides (e.g. strontium) (Dentz et al., 2011; Kapetas et al., 2014; Neuman and Tartakovsky, 2009). With respect to reactive transport it should be mentioned, that separation of migration and sorption into independent sets of measured/fitted parameters is not justifiable, although such separation has been used in the traditional ADE formulation (Rubin et al., 2012). This makes the prediction of reactive nuclide transport with pervasive non-Fickian phenomenon even more challenging. Thus, for a special reactive species, strontium in this study, there is a continuing need to advance the understanding and prediction of transport phenomena involving natural tracer release, non-Fickian migration and sorption.

The objectives of this paper are: (1) to re-analyse BTCs from column experiments simulating rainfall infiltration scenarios and transport behaviour of strontium (Gaohua et al., 2013); (2) to apply the ADE and CTRW models to characterize coupled effects of release, transport and sorption processes; (3) to identify transport parameters by inverse modelling against experimental data; (4) to evaluate the applicability of ADE and CTRW models in capturing reactive species transport with pervasive non-Fickian transport. This study advances the understanding and prediction of radionuclide transport through heterogeneous systems, which is critical for environmental remediation of contaminated sites and the safety assessment of nuclear waste subsurface disposal.

2. Methodology

2.1. Column experiments

Safety assessment of near-surface zone and planning remedial options for contaminated sites require detailed studies of release and transport processes. Of particular interest for near-surface nuclear waste storage is the radioactive fallout dispersed to surface in a rainfall scenario. The column experiments described here served this purpose. These were mocking rainfall infiltration with a contaminant (source) located at the inlet and slowly released to the environment, rather than the traditional supply of a tracer concentration through columns over time. Firstly, examining the tracer concentrations leaching from the source layer is essential for identifying and then modelling the inlet condition. Secondly, measuring the tracer mass eluted from the columns is necessary for the quantitative analysis of mass transport and models validation.

Column experiments, with setup shown in Fig. 1, were performed to investigate strontium (Sr) transport with varying sprinkling volumetric flow rates, and different packed materials, including sand and clay. Bromine (Br) was used as a conservative tracer for water flow. Full details of the experimental setup and primary results are described by Gaohua et al. (2013); only information relevant to this work is given below.

The tracer experiments were conducted in a set of cylindrical organic glass columns (3cm diameter and 20cm length) packed with sand and/or clay. Eight different columns were prepared: columns a, b, c, d were 18-cm long packed by medium sand of 0.25～0.50mm diameter; columns e, f, g, h were packed by a mixture of clay and the same sand with 25%, 50%, 75% and 100% clay content, respectively. The packing materials were taken from the sediments in northwest China. Neat tracer sources were prepared by the following the steps: (1) Sr stock solution was made by dissolving 100g $SrCl_2 \cdot 6H_2O$ into 250mL distilled water; Br stock solution was made by dissolving 66g NaBr in 1000mL distilled water; and (2) 250g pure quartz sand was placed in 1000mL beaker, to which 105mL Sr solution and 50mL Br solution were added, respectively; Beaker was stirred well and dried until moisture content reduced to 3%.

Columns a-d were sprinkled with distilled water under different volumetric flow rates: 100mL/d, 50mL/d, 20mL/d and 2mL/d, respectively. We note that although a-d were packed with sand with the same particle size distribution, the packing structure might have varied due to preparation uncertainty. Columns e-h were sprinkled with the same flow rate 2mL/d of distilled water. To prevent water and soil loss, a polyester fibre membrane with an aperture 0.45μm was placed at the bottom of column. Sprinkling volumetric flow rate was controlled by injection pump and peristaltic pump as a water supply device.

During experiments, columns were saturated slowly by leaching with distilled water until steady-state fluid velocity was achieved. The first inlet section was occupied by a 0.8-cm thick tracer source layer (Br 135.5mg and Sr 718mg, approximately), which was overlain by a 0.5cm thick sand. At the column outlet, effluent water was collected automatically over experimental duration. The concentration of Br and Sr was determined by ion chromatography and inductively coupled plasma-atomic emission spectrometry (ICP-AES), respectively. Thus, the breakthrough curves (temporal profile of concentration) of Br and Sr were obtained.

147 2.2. Transport model with Advection-Dispersion Equation (ADE)

148 Assuming steady-state flow in homogeneous porous media, the classical ADE for one-dimensional
149 transport of species, subject to equilibrium isotherm adsorption and radioactive decay, can be written
150 as (Šimůnek et al., 1999; Toride et al., 1995)

151 $$R\frac{\partial C}{\partial t} = D\frac{\partial^2 C}{\partial t^2} - v\frac{\partial C}{\partial x} - \lambda C\,, \tag{1}$$

152 where C is species concentration in the liquid (ML^{-3}), R is dimensionless retardation factor, D is
153 dispersion coefficient (L^2T^{-1}), v is average pore water velocity (LT^{-1}), λ is the first-order decay
154 coefficient (T^{-1}), t is time (T), and x is transport distance (L). R depends on the relative transport
155 velocity, v_s, such that $R = v / v_s$, and reflects the strength of sorption, $R = 1$ when no sorption occurs.
156 D can be represented by $D = v\alpha + \tau D_w$ (Bear, 1972), where D_w is molecular diffusion coefficient in
157 free water (L^2T^{-1}), α is dispersivity (L), τ is a dimensionless tortuosity factor. For stable species $\lambda = 0$.

158 For an initially species-free and semi-finite column, where tracer is placed in a fixed layer at the
159 inlet of column and is eluted with free water, the leach concentration of effluent will decrease over
160 time as the tracer mass in the source layer reduces due to mass loss through leaching. The leach
161 concentration can be estimated via an exponential function using the leaching rate coefficient (Chen
162 et al., 2007)

163 $$C(t,0) = \frac{\lambda_L m_0}{Q} \mathrm{e}^{-(\lambda_L + \lambda)t} \tag{2}$$

164 where $C(t,0)$ is the leach concentration (ML^{-3}), m_0 is the total mass of tracer (M), Q is the sprinkling
165 volumetric flow rate (L^3T^{-1}), λ_L is a leaching rate coefficient (T^{-1}). A first-order decay rate of the
166 source term, similar to radioactive decay, was given by (Baes and Sharp, 1983; Chen et al., 2007)

167 $$\lambda_L = \frac{Q}{\varepsilon R V_t} = \frac{I}{\varepsilon R d} \tag{3}$$

where ε ,V_t ,d are effective porosity (L^3L^{-3}), volume (L^3), and depth (L) of the tracer source layer, respectively, I is infiltration rate of water (LT^{-1}), R is the retardation factor of tracer in the source layer (-).

The model of leach concentration represented by Eqs.(2)~(3) is a relatively simple approximation of the complex transport mechanism involving physical and chemical processes. This model assumes that equilibrium adsorption is achieved instantaneously between the passing water and the source layer when the percolating water comes into contact with the tracer source layer. The equilibrium is generally described by a linear adsorption relationship using a distribution coefficient (K_d) estimated from batch experiments (Baes and Sharp, 1983; Chen et al., 2007). R can be thus calculated based on K_d, such that $R=1+\rho_b \cdot K_d/n_e$, where ρ_b is bulk density, n_e is effective porosity. Moreover, combining with the inverse modelling, R can be obtained directly from column experiments (Rod et al., 2010).

The simulated BTCs can be solved with given boundary conditions. Here, Dirichlet boundary with prescribed concentration, which is determined by the leach concentration curve as described by Eq.(2), is set for the inlet boundary of the column. Further, Neuman boundary condition with prescribed flux is set for the outlet boundary.

2.3. Transport model with Continuous Time Random Walk (CTRW)

The concept and the formulation of the CTRW method can be found in various references (e.g. Berkowitz et al., 2006; Cortis et al., 2004; Dentz et al., 2004; Edery et al., 2015; Edery et al., 2013; Neuman and Tartakovsky, 2009; Scher and Lax, 1973). Here, we sketch the key features of CTRW for the purpose of this study.

In the CTRW framework, transport processes are conceptualized as a series of particle transitions by statistically characterizing tracer motion. The main feature of CTRW lies in quantifying temporal transition probability of particle transport induced by spatial heterogeneities via a memory function (Berkowitz et al., 2006).

The one-dimensional (1D) CTRW for macroscopic transport through a uniform domain is given in Laplace space by Eqs. (4)-(7) (Cortis and Berkowitz, 2005; Edery et al., 2014)

$$u\tilde{c}(x,u) - c_0(x) = -\tilde{M}(u)\left[v_\psi \frac{\partial}{\partial x}\tilde{c}(x,u) - D_\psi \frac{\partial}{\partial x^2}\tilde{c}(x,u) \right] \quad (4)$$

$$\tilde{M}(u) \equiv \bar{t}u \frac{\tilde{\psi}(u)}{1-\tilde{\psi}(u)} \quad (5)$$

$$v_\psi = \frac{1}{n\bar{t}} \sum_s p(s)s \quad (6)$$

$$D_\psi = \frac{1}{n\bar{t}} \sum_s \frac{1}{2} p(s)ss \quad (7)$$

where u is the Laplace variable and the tilde represents the Laplace transformed variable; c_0 is the initial concentration and $\tilde{c}(x,u)$ is the Laplace–transformed normalized concentration; $\tilde{M}(u)$ is a memory function; $\psi(t)$ is a probability density function (PDF), defined as the probability rate for a transition time t between transport sites and $\tilde{\psi}(u)$ is the Laplace–transformed form of $\psi(t)$; v_ψ and D_ψ are the tracer transport velocity and dispersion coefficient, respectively; $\bar{t}$ is a characteristic time; n is porosity, and $p(s)$ is the probability distribution of the length of transitions. Note that both v_ψ and D_ψ depend on $\psi(t)$, which is fundamentally different from the average pore water velocity (v) and dispersion coefficient (D) in the classical ADE (Berkowitz et al., 2006).

The PDF, $\psi(t)$, is the core of the CTRW formulation as it depicts the nature of solute plume migration patterns (Berkowitz et al., 2001). Depending on the choice of $\psi(t)$, the CTRW can capture a broad range of transport regimes, including the transition from non-Fickian to Fickian transport. There are several compelling forms of $\psi(t)$ that have been proposed in the literature (Berkowitz et al., 2006; Cortis and Berkowitz, 2005; Cortis et al., 2004; Margolin et al., 2003). Here, we present one specific form for conservative tracer transport, which is widely used to interpret transport phenomena at different scales: the truncated power law (TPL) model

$$\tilde{\psi}(u) \equiv (1+\tau_2 u t_1)^\beta \exp(t_1 u)\Gamma(-\beta, \tau_2^{-1} + t_1 u) / \Gamma(-\beta, \tau_2^{-1}), 0 < \beta < 2 \quad (8)$$

where β is a critical parameter characterizing the regimes of the dispersive transport, t_1 is a characteristic transition time for the onset of the power law region, t_2 is a "cut-off" time, $\tau_2 = t_2 / t_1$. The memory function is determined by setting $\bar{t} = t_1$.

The TPL model allows for a systematic investigation of non-Fickian transport observed for transition times $t_1 < t < t_2$, and for analysing the transition from non-Fickian to Fickian transport for $t > t_2$ (Dentz et al., 2004). The t_1 sets the lower limit from which the power law behaviour begins, so that the time range of interest is $t > t_1$. The time t_2 governs the crossover from power law to a decreasing exponential function (Edery et al., 2014; Gao et al., 2009). Overall, the $\psi(t)$ exhibits a wide change in behaviour as a function of β that largely determines $\psi(t)$ (Edery et al., 2014). That is, β controls the particle transport and thus functionally captures the dispersion regimes (i.e. Fickian or non-Fickian) (Cortis et al., 2004). The relative shapes of the anomalous transport regimes are strongly dependent on β, as shown in Table 1.

In this study, the TPL model is used to interpret the measured BTCs of strontium, since the TPL model has been proved to be effective in describing non-Fickian transport for numerous laboratory and field observations (Edery et al., 2014). Specifically, the Laplace transformed analytical solution to the CTRW equations is obtained for a set of given boundary conditions: Dirichlet boundary condition (prescribed concentration) with an exponential decay function of concentration is specified at the inlet of the columns according to the Eq.(2); Neumann (prescribed flux) boundary condition is specified at the outlet boundary.

2.4. Inverse modelling with ADE and CTRW-TPL methods

The experimental BTCs are analyzed using the equilibrium ADE and CTRW-TPL methods described above. Inverse modelling for parameters identification is implemented by fitting analytical solutions with the models to the observed BTCs. The inversion processes are conducted through the non-linear least squares inversion program, CXTFIT (Šimůnek et al., 1999; Toride et al., 1995), and

240 the CTRW MATLAB toolbox which is available from the website
241 http://www.weizmann.ac.il/ESER/People/Brian/CTRW.

242 From the measured effluent concentration C_f at the outlet boundary, and the concentration at the
243 onset of leaching process C_0 (both in ML^{-3}), a normalized concentration is defined by

244 $$c = \frac{C_f}{C_0}, \tag{9}$$

245 Further, the ratio of eluted tracer mass to the total tracer mass m_0, i.e. the cumulative mass fraction
246 eluted from columns is calculated by

247 $$f = \frac{Q\int_0^t C_f dt}{m_0}. \tag{10}$$

248 The two parameters, c and f, are used to constrain the inversion process.

249 The inverse modelling with the equilibrium ADE for bromide (Br) and strontium (Sr) is performed
250 with CXTFIT. The inverse problem is solved by minimizing an objective function of root mean
251 square error between observed and fitted concentrations (Šimůnek et al., 1999). For bromide, the
252 retardation coefficient R is set to 1, because it is assumed that bromide ions have minimal sorption
253 onto sand and clay (Srinivasan and Sarmah, 2014). The parameters identified for Br, v and D, are
254 then used as input values for the measured strontium BTCs, so that R for strontium can be estimated.

255 Further, the inversion of 1D TPL model for strontium is implemented by comparing the predicted
256 BTCs from the CTRW to the normalized BTCs from tracer experiment. The inverse modelling
257 requires initial guesses of seven fitted parameters, including v_ψ, D_ψ, β, t_1, t_2, Λ and α. Depending on
258 how close the initial values of the parameters are to the optimized ones, the inverse estimation of
259 parameters can be time-consuming. Here the values of v and D from CXTFIT are used as initial
260 guesses of v_ψ and D_ψ. Considering that the TPL model is sensitive to the exponent β while relatively
261 insensitive to t_1 and t_2 (Cortis and Berkowitz, 2005), a broad range for β is tested, from 0.8 to 1.8,
262 while t_1 and t_2 are estimated from global error minimisation. Further, Λ and α, which influence the

263 degree of retardation and the power law slope of the BTC tailing (Cortis et al., 2006; Margolin et al.,
264 2003), are initially set to 0.01~0.3 and 0.01~0.2, respectively. The approach to estimate initial values
265 and to perform adjustments using trial and error method corresponds to the successful sensitivity
266 analysis by Cortis et al.(2006). This allowed for achieving good agreement between experimental
267 and modelling results with the CTRW toolbox.
268
269 **3. Results and Discussion**
270 3.1. Tracer leach concentration and eluted mass fraction
271 Leach concentration of bromine and strontium in the experiments are estimated by Eqs. (2) and (3),
272 and presented in Fig. 2. Assuming that there is no strontium sorption to quartz in the source layer
273 (Rod et al., 2010), strontium concentration demonstrates an exponential decay over the experimental
274 duration, similar to bromine. Because the leaching rate, λ_L, is proportional to the volumetric flow rate,
275 Q, the leach concentration is inversely exponentially dependent on Q, i.e. very strongly. The higher
276 the flow rate is, the more easily the tracer particles transfer to aqueous phase and are subjected to
277 stronger hydrodynamic dispersion with time. This eventually leads to faster falloff of leach
278 concentration with shorter residence time, and vice versa (Fig. 2). Moreover, as more mass of
279 strontium than bromine is located at the source layer, the strontium concentration is greater than that
280 of bromine at the onset of leaching. The release of source term is characterized as a continuous and
281 decreasing process rather than an instantaneous process. This is due to mass loss through leaching
282 over time. As a result, the inlet condition of the leaching release process should be treated as an
283 exponential decay function, instead of a simple instantaneous pulse or Dirac delta function, which is
284 commonly employed for experimental and numerical simplicity. This treatment of tracer release is
285 closer to the natural condition in simulating rainfall infiltration, and is critical for dynamic simulation
286 of tracer transport, e.g. in the CTRW modelling.

The cumulative eluted mass fraction for bromine is approximately 39%~58% for the observed columns, as given in Fig. 3. The results show that around half of the mass remains in the source layers and soil columns. This indicates that a fraction of pore water is immobile due to the presence of "dead pore" in relation to fluid flow. For strontium, the cumulative eluted mass fraction is approximately 16%~49% (Fig. 3), which is much less than that of bromine. This demonstrates that, in addition to the effect of immobile water on mass transport (i.e. diffusion into immobile zones), the sorption of strontium on clay minerals is significant and results in extra mass loss as it is transported through packed columns. Expectedly, more clay content results in larger sorption of strontium and less aqueous strontium, as seen for columns e-h. The effect of volumetric flow rate on transport is excluded in the study since the packing structures for columns a-d may vary from one to another due to uncertainty in the experimental design. It is worth noting, however, that larger eluted mass fraction is observed for bromide and strontium in column d, which can be attributed to relatively larger heterogeneity in this packing resulting in local preferential flows and non-Fickian transport, as discussed in the next sub-section.

3.2. Observations of non-Fickian transport

The typical non-Fickian features, asymmetric BTCs with early breakthrough and late tailings, are observed in varying degrees in our study. Particularly pronounced is the experiment with column d. This is illustrated by the concentration results shown in Fig. 4, which are also used to show the predictions of the two methods after parameter estimation, i.e. best fits. Although column d is packed with "homogeneous" sand and sprinkled with a relatively slow flow rate, 2mL/d, the "anomalous" transport phenomenon is remarkable. This might be due to the occurrence of preferential flow path caused by the heterogeneous packing structure. Nevertheless, non-Fickian transport of strontium is observed in all BTCs, which implies that physical-chemical heterogeneities contribute strongly via preferential flow, diffusion in/out of immobile zones and complex sorption.

312 The estimated parameters of the two tested models are given in Table 2. Estimated $0 < \beta < 1$ for
313 columns d, g, and h, indicates highly dispersive transport leading to longer tailing. The early
314 breakthrough time observed for column d (Fig. 4d) is not expected in view of the lower flow rate
315 compared to columns a-c. This suggests the existence of stronger preferential flow path as well as
316 larger immobile zones. Potentially, a fraction of strontium is trapped or diffuses into low
317 permeability lenses and remains there for long times. The strontium particles that firstly reach the
318 outlet with short residence time are those that propagate through the faster moving regions along
319 preferential flow paths. Thus, the "homogeneous" column d with a much smaller β, larger transport
320 velocity and dispersion coefficient, fails to comply with the Fick transport theory and exhibits
321 significant non-Fickian dispersion.

322 For columns g and h (Fig. 4g and h), in addition to diffusion into immobile zones, sorption is a
323 reasonable explanation for the non-Fickian migration based on the conclusion of Rubin et al. (2012).
324 The reduction and delay of the peak concentration and the tailing features are affected by the
325 additional processes of adsorption/desorption of strontium onto/from the mineral surface. This
326 partitioning mechanism between aqueous and mineral phases enhances the non-Fickian transport and
327 causes the failure of Fickian-based equilibrium ADE model.

328 Comparatively, columns a, e and f with $1 < \beta < 2$, present moderate non-Fickian processes at
329 different water flow fields and particles residence time. Note that in Fig. 4a, the BTCs demonstrate
330 early arrival and late tail, corresponding to the larger transport velocity and dispersion coefficient,
331 which are similar to the phenomenon of column d and distinct from columns e and f. This can be
332 explained by the higher pore water velocities enhancing the preferential flow in the presence of
333 immobile water (Gaber et al., 1995; Li and Ren, 2009). For columns e and f, sorption retardation
334 process (e.g. strontium cations exchange with inorganic cations in clay), serves as an additional
335 factor contributing weakly to the non-Fickian dispersive transport. The contribution of sorption to the
336 non-Fickian features depends on the amount of clay as seen in Fig. 4e-h.

337 Unlike column a with high volumetric flow rate, Fickian transport at medium volumetric flow rate
338 is predicted fairly well for column b and c with values of β slightly larger than 2 (Fig. 4b and c). This
339 suggests that the assumption of equilibrium mass transfer between spectrums of different mobility is
340 adequate for moderate flow rates within relatively homogeneous structures. The results also supports
341 our assumption that little sorption/desorption occurs for sand-packed columns.
342 Our results strengthen the understanding that both physical and chemical heterogeneities may
343 influence strongly species transport (Mohamed et al., 2010). For laboratory scale disturbed and
344 undisturbed soil columns, the role of physical non-equilibrium transport stemming from physical
345 heterogeneities, i.e. different pore scale structures, is critical for inducing non-Fickian phenomena:
346 macro-pores commonly control the preferential flow process, while some pore spaces serve as tracer
347 sinks at early times, and then release tracer slowly. This drives non-Fickian transport with late tailing
348 feature (Dousset et al., 2007; Swanson et al., 2015). It is known that preferential flow and transport
349 may exist in unconsolidated sandy soils. This applies to soils with available structural voids as a
350 result of textural shift horizontally, funneling effect, or fluid instabilities due to viscosity or density
351 differences between the invading and resident water (Kamra et al., 2001). Further, chemical
352 heterogeneities across various scales, which control chemical equilibrium (instantaneous sorption) or
353 non-equilibrium (kinetic sorption) transport processes, apparently contribute the non-Fickian
354 mechanisms.
355
356 3.3. Physical heterogeneity effects on non-Fickian transport
357 Due to minimal sorption in the sand-packed columns, column experiments a-d allow for
358 evaluating transport behaviour quantitatively due to physical aspects alone – advection and
359 dispersion. The main parameters influencing advective-dispersive transport are the fluid velocity and
360 dispersion coefficient. Although a correlation between the tracer transport velocities and the
361 volumetric flow rates is found by the ADE model (Table 2), the resultant fitting parameters do not

follow the expected Fickian trend, because the ADE is insufficient to capture the highly non-Fickian transport in column d. In contrast, transport velocity and dispersion coefficient for column d estimated by the CTRW-TPL are greater than those for columns b and c. This implies that columns b and c are likely forming more homogeneous packed structures, while column d is likely to have a relatively heterogeneous one. That is, the presence of macro-pores in column d may lead to overall faster transport and high dynamic dispersion.

Similar to fracture-matrix systems, where fracture leads to fast breakthrough and matrix contributes to the long tailing of BTCs (Kosakowski and Smith, 2005), the eluted mass fraction and inverse modelling for the BTCs indicate that the presence of interconnected open channels, e.g. macro-pores or preferential flow paths, in conjunction with low velocity regions, e.g. in dead-end channels or immobile zones, is responsible for the non-Fickian dispersion transport in heterogeneous columns. Specifically, local flow velocity variations, i.e. low-velocity fluid near channel walls and higher-velocity fluid near the centre of the channel, as well as the matrix diffusion, result in a skewed breakthrough curve with an earlier peak and longer tail.

Pore-scale heterogeneity and variations of fluids velocity in the pore space are known to yield enhanced dispersive transport, associated with the Peclet number (*Pe*) (Dentz et al., 2011). Depending on the selected length scale, *Pe* is presented in different forms (Bear and Cheng, 2010). At the macroscopic level, $Pe = v L / D = L / \alpha$, where L is a characteristic length, represents the ratio between the advective and dispersive transport terms. It increases when the advection dominates over dispersion (Šimůnek et al., 2008). For $Pe << 1$, the advective mass flux may be neglected as much smaller than the dispersive one, and vice versa (Bear and Cheng, 2010). In this study, based on the fitted parameters (Table 2) and the column length, L = 18cm, *Pe* is calculated for the experimental columns with results presented in Table 3. The results, $1 < Pe < 200$, show that both dispersion and advection are operating, e.g. there is a transition region to a power-law regime (Dentz et al., 2011).

In this case, the CTRW-based TPL model is valid for transport regimes. The possible effects of *Pe* on dispersive transport are not analysed here, but are subject of further investigations.

3.4. Chemical heterogeneity effects on non-Fickian transport

The column experiments e-h are designed to evaluate the effect of sorption on strontium transport. Expectedly, the tracer transport velocities decrease with increased clay content (Table 2), as strontium transport is significantly retarded. The emergent behaviour is non-Fickian dispersive transport, i.e. reduction and delay of the peak concentration and elongation of tailing. The larger the clay content, the greater the retardation and the reduction of strontium (Fig. 4e-h, Table 2). Inversely, the degree of non-Fickian transport is negatively associated with clay content (see Tables 1 and 2). Those phenomena are fundamentally due to the sorption/desorption of strontium on clay surface.

Sorption coefficients, represented in the form of R or K_d, are commonly used to approximate the extent of species sorption on various minerals, where typical sorption reactions are surface complexation and ion exchange (Altmann et al., 2001). As sorption is commonly a complex function of chemical properties, e.g. pH, ionic strength, mineral surface area, etc., the integral (constant) coefficient R or K_d used in ADE model often fail to capture such complexities. This is demonstrated by our results that the equilibrium ADE is insufficient to fully capture measured BTCs. Moreover, for spatially heterogeneous retardation properties, which can give rise to distinct non-Fickian transport behaviours, the sorption coefficient R may not exist at relevant time and length scales (Dentz and Castro, 2009). Consequently, the prediction of increasing R with increasing clay content by the ADE model (Table 2) is not sufficient to describe strontium transport in clayed media using the equilibrium sorption model (Fig. 4e-h), because R reflects the simplified kinetic sorption process to some degree but fails to capture the chemical heterogeneities, e.g. spatially varying sorption properties and specific reactive surface areas (Dentz et al., 2011).

In contrast, the CTRW framework with a sticking rate term is found capable of representing strontium transport (Fig. 4e-h), where slow and fast species transport is manipulated by the random spatial and time increment as a stochastic process, and heterogeneity is mapped on the joint distribution of transition length and times (Dentz et al., 2011). As expected, the average "sticking" rate Λ increases with increasing clay content (Table 2). This demonstrates that Λ represents physically the degree of sorption of strontium on clay minerals, and shows that our CTRW-TPL model is robust in capturing non-Fickian transport when sorption is operating (Fig. 4e-h). Overall, the CTRW model is of the greater flexibility to describe the local scale transport with spatially varying equilibrium mass transfer and sorption-desorption reactions (Bromly and Hinz, 2004; Dentz and Castro, 2009), and thus can capture observed non-Fickian transport features, e.g. highly non-Gaussian BTCs.

3.5. Performance of ADE and CTRW methods in environmental modelling

Environmental modelling uses mathematics and computers to simulate physical and chemical phenomena across different environmental scales (Holzbecher, 2012). For nuclide transport related to contaminated sites remediation and safety assessments of a nuclear waste disposal, a number of macroscopic models based on ADE have been proposed, e.g. dual-porosity model, dual permeability model, two-phase model (Kapetas et al., 2014; Šimůnek and van Genuchten, 2008). The CTRW framework has mainly been applied for reactive transport, e.g. chemical sorption on minerals (Deng et al., 2013; Dentz et al., 2011; Edery et al., 2015).

In this work, inverse modelling by CXTFIT and CTRW toolbox have been used to obtain the relevant model parameters (Table 2). Overall, the CTRW performs better than the ADE, specifically in capturing measured BTCs, even though there should be little difference between them for column d, due to negligible sorption (Fig. 4). The equilibrium ADE modelling leads to broad range of parameters in capturing asymmetric BTCs by CXTFIT (Table 2), as the simple average deterministic

values may be insufficient to capture pervasive non-Fickian transport and estimate the randomness of tracer transference. The CTRW-TPL model appears to be the preferred method to describe this non-Fickian transport. Further, the CTRW-TPL is found insensitive to the magnitude of the Peclet number and offers an efficient alternative for modelling species transport in convection-dominant flows (COMSOL, 2013). It is noted that some BTCs fitted with the ADE through CXTFIT are similar to ones with TPL through CTRW toolbox (Fig. 4). This can be explained by the relative flexibility of CXTFIT to fit certain BTCs. However, this flexibility appears to have limited validity, excluding strongly preferential flow conditions (Kamra et al., 2001).

Both ADE and CTRW methods have been widely credited as effective tools to simulate species transport in heterogeneous conditions, utilising Lagrangian (particle tracing) and Eulerian (integral-differential equation) frameworks (Bakshevskaia and Pozdniakov, 2015; Hansen and Berkowitz, 2015; Rumynin, 2011). In fact, CTRW offers a general formalism which encompasses the ADE models, and thus has comprehensive ability in treating non-Fickian dispersion transport (Berkowitz et al., 2006; Gao et al., 2009). Moreover, the probabilistic base of CTRW provides a more realistic mathematical framework to model the advection-dispersion in porous media than the deterministic base of ADE (Kulasiri, 2013). However, there are unresolved issues with respect to the non-uniqueness of fitted parameters and inverse solution because of internal correlations between CTRW parameters. This results in the existence of many local minima in the parameter estimation method (Kulasiri, 2013). To surmount the problem, apart from collecting supplementary information which is independent of the fitted parameter and reflects the actual migration processes, it is suggested to integrate the ADE and CTRW approaches to find optimal parameters to improve inversion problem. For example, in this work we set admissible limits to the effective transport velocity and dispersion coefficient found by ADE model as constraints to the CTRW. Then, in the CTRW framework, β can be estimated through analysis of the velocity field (Gao et al., 2009). Finally, the optimization scheme allows for calculating reliable parameter values, which provide robust model prediction.

From a practical perspective, however, a disadvantage of CTRW is the lack of well-established public domain or commercial package; only CTRW MATLAB toolbox is available as mentioned in the section 2. In contrast, there are widely available user-friendly software packages for ADE, such as CTXFIT, HYDRUS (Šimůnek et al., 2008), MODFLOW (Chiang and Kinzelbach, 2005), upon which customized models can be built without sophisticated programming and coding.

4. Conclusions

Understanding release and transport of radioactive strontium is important in the context of remedial options for contaminated sites and safety assessment of disposal in near-surface zone. Few investigations have focused on strontium non-Fickian transport with coupled advection, dispersion and sorption processes, through an integrated approach of laboratory dynamic column experiments and computer modelling. By re-analyzing BTCs from realistic column experiments of strontium transport behaviour, comprehensive analysis for release and non-Fickian dispersive migration of strontium was carried out using the ADE-based CTXFIT and TPL-based CTRW toolbox. The results allow for the following conclusions:

(1) Tracer release is found to be exponentially decaying from experimentally-informed understanding that it is a continuous and decreasing process (Fig. 2); this is essential for defining appropriate inlet conditions in future modelling.

(2) Observed reduction of eluted tracer mass (Fig. 3), 39%~58% of bromine and 16%~49% of strontium, results from heterogeneities in the physical and chemical properties and processes: molecular diffusion into/out immobile zone, strong preferential flow paths, sorption on the clay surface, etc; this leads to non-Fickian behaviour with variable strength shown by early breakthroughs and late tails.

(3) The CTRW-TPL model can capture non-Fickian transport with $0 < \beta < 2$ and Fickian transport with $\beta > 2$ (Table 2, Fig. 4). The non-Fickian dispersive transport is due to variation of flow fields and sorption retardation processes.

(4) The CTRW-TPL performs better than the ADE model in terms of capturing pervasive non-Fickian transport, however, both ADE and CTRW models have positive and negative aspects for practical use: integration of ADE and CTRW is suggested to obtain reliable parameters and provide robust model prediction for both conservative and reactive transport.

Acknowledgments

This research reported here was partially funded by the Project of Intelligence Importation from Northwest Institute of Nuclear Technology (NINT) of China. We would like to express our sincere appreciations to Prof. Brian Berkowitz for many useful discussions and kindly help in CTRW application.

References

Baes, C., Sharp, R., 1983. A proposal for estimation of soil leaching and leaching constants for use in assessment models. Journal of Environmental Quality, 12(1): 17-28.

Bakshevskaia, V.A., Pozdniakov, S.P., 2015. Simulation of Hydraulic Heterogeneity and Upscaling Permeability and Dispersivity in Sandy-Clay Formations. Mathematical Geosciences: 1-20.

Bear, J., 1972. Dynamics of fluids in porous media. Courier Corporation.

Bear, J., Cheng, A.-D., 2010. Modeling groundwater flow and contaminant transport, 23. Springer Science & Business Media.

Bencala, K.E., 1984. Interactions of solutes and streambed sediment: 2. A dynamic analysis of coupled hydrologic and chemical processes that determine solute transport. Water Resources Research, 20(12): 1804-1814.

508 Berkowitz, B., Cortis, A., Dentz, M., Scher, H., 2006. Modeling non-Fickian transport in geological
509 formations as a continuous time random walk. Reviews of Geophysics, 44(2).
510 Berkowitz, B., Kosakowski, G., Margolin, G., Scher, H., 2001. Application of continuous time
511 random walk theory to tracer test measurements in fractured and heterogeneous porous
512 media. Groundwater, 39(4): 593-604.
513 Berkowitz, B., Scher, H., 2009. Exploring the nature of non-Fickian transport in laboratory
514 experiments. Advances in Water Resources, 32(5): 750-755.
515 Bijeljic, B., Blunt, M.J., 2006. Pore-scale modeling and continuous time random walk analysis of
516 dispersion in porous media. Water Resources Research, 42(1).
517 Bijeljic, B., Muggeridge, A.H., Blunt, M.J., 2004. Pore-scale modeling of longitudinal dispersion.
518 Water Resources Research, 40(11).
519 Bijeljic, B., Raeini, A., Mostaghimi, P., Blunt, M.J., 2013. Predictions of non-Fickian solute
520 transport in different classes of porous media using direct simulation on pore-scale images.
521 Physical Review E, 87(1): 013011.
522 Blunt, M.J. et al., 2013. Pore-scale imaging and modelling. Advances in Water Resources, 51: 197-
523 216.
524 Bromly, M., Hinz, C., 2004. Non-Fickian transport in homogeneous unsaturated repacked sand.
525 Water Resources Research, 40(7).
526 Bruno, J., Duro, L., Grivé, M., 2002. The applicability and limitations of thermodynamic
527 geochemical models to simulate trace element behaviour in natural waters. Lessons learned
528 from natural analogue studies. Chemical geology, 190(1): 371-393.
529 Bugai, D. et al., 2012. Radionuclide migration at experimental polygon at Red Forest waste site in
530 Chernobyl zone. Part 2: Hydrogeological characterization and groundwater transport
531 modeling. Applied Geochemistry, 27(7): 1359-1374.

Chen, Q., Kowe, R., Mobbs, S., Jones, K., 2007. Radiological Assessment of Disposal of Large Quantitites of Very Low Level Waste in Landfill Sites. Health Protection Agency, Radiation Protection Division.

Chiang, W.-H., Kinzelbach, W., 2005. 3D-groundwater modelling with PMWIN, a simulation system for modelling groundwater flow and transport. Springer, New York.

COMSOL, I., 2013. Particle Tracing Module Model Library Manual. http://hpc.mtech.edu/comsol/pdf/Particle_Tracing_Module/ParticleTracingModelLibraryManual.pdf

Cortis, A., Berkowitz, B., 2004. Anomalous transport in "classical" soil and sand columns. Soil Science Society of America Journal, 68(5): 1539-1548.

Cortis, A., Berkowitz, B., 2005. Computing "anomalous" contaminant transport in porous media: The CTRW MATLAB toolbox. Groundwater, 43(6): 947-950.

Cortis, A., Gallo, C., Scher, H., Berkowitz, B., 2004. Numerical simulation of non-Fickian transport in geological formations with multiple-scale heterogeneities. Water Resources Research, 40(4).

Cortis, A. et al., 2006. Transport of Cryptosporidium parvum in porous media: Long-term elution experiments and continuous time random walk filtration modeling. Water resources research, 42(12).

Deng, H. et al., 2013. Upscaling retardation factor in hierarchical porous media with multimodal reactive mineral facies. Chemosphere, 91(3): 248-257.

Dentz, M., Castro, A., 2009. Effective transport dynamics in porous media with heterogeneous retardation properties. Geophysical Research Letters, 36(3).

Dentz, M., Cortis, A., Scher, H., Berkowitz, B., 2004. Time behavior of solute transport in heterogeneous media: transition from anomalous to normal transport. Advances in Water Resources, 27(2): 155-173.

557 Dentz, M., Le Borgne, T., Englert, A., Bijeljic, B., 2011. Mixing, spreading and reaction in
558 heterogeneous media: A brief review. Journal of contaminant hydrology, 120: 1-17.
559 Detwiler, R.L., Rajaram, H., Glass, R.J., 2000. Solute transport in variable-aperture fractures: An
560 investigation of the relative importance of Taylor dispersion and macrodispersion. Water
561 Resources Research, 36(7): 1611-1625.
562 Eagling, J., Worsfold, P.J., Blake, W.H., Keith-Roach, M.J., 2013. Fate of 90 Sr and U (VI) in
563 Dounreay sediments following saline inundation and erosion. Chemosphere, 92(8): 911-917.
564 Edery, Y., Dror, I., Scher, H., Berkowitz, B., 2015. Anomalous reactive transport in porous media:
565 Experiments and modeling. Physical Review E, 91(5): 052130.
566 Edery, Y., Guadagnini, A., Scher, H., Berkowitz, B., 2013. Reactive transport in disordered media:
567 Role of fluctuations in interpretation of laboratory experiments. Advances in Water
568 Resources, 51: 86-103.
569 Edery, Y., Guadagnini, A., Scher, H., Berkowitz, B., 2014. Origins of anomalous transport in
570 heterogeneous media: Structural and dynamic controls. Water Resources Research, 50(2):
571 1490-1505.
572 EPA, 2015. Radiation Protection Reference Information-Strontium.
573 http://www.epa.gov/radiation/radionuclides/strontium.html updated on June 29, 2015.
574 Gaber, H., Inskeep, W., Wraith, J., Comfort, S., 1995. Nonequilibrium transport of atrazine through
575 large intact soil cores. Soil Science Society of America Journal, 59(1): 60-67.
576 Gao, G., Zhan, H., Feng, S., Huang, G., Mao, X., 2009. Comparison of alternative models for
577 simulating anomalous solute transport in a large heterogeneous soil column. Journal of
578 hydrology, 377(3): 391-404.
579 Gaohua, S., Xu, Y.J.L.D.Z., Zhiqian, H., 2013. The column experiment and numerical simulation for
580 nuclide migration. Environmental Chemistry, 3: 024.

581 Hansen, S.K., Berkowitz, B., 2015. Integrodifferential formulations of the continuous-time random
582 walk for solute transport subject to bimolecular A+ B→ 0 reactions: From micro-to
583 mesoscopic. Physical Review E, 91(3): 032113.
584 Holzbecher, E., 2012. Environmental modeling: using MATLAB. Springer Science & Business
585 Media.
586 Hull, L.C., Schafer, A.L., 2008. Accelerated transport of 90 Sr following a release of high ionic
587 strength solution in vadose zone sediments. Journal of contaminant hydrology, 97(3): 135-
588 157.
589 Kapetas, L., Dror, I., Berkowitz, B., 2014. Evidence of preferential path formation and path memory
590 effect during successive infiltration and drainage cycles in uniform sand columns. Journal of
591 contaminant hydrology, 165: 1-10.
592 Kosakowski, G., Smith, P., 2005. Modelling the transport of solutes and colloids in the Grimsel
593 migration shear zone, Paul Scherrer Institut, CH-5232 Villigen PSI (Switzerland).
594 Kulasiri, D., 2013. Non-fickian Solute Transport in Porous Media: A Mechanistic and Stochastic
595 Theory. Springer.
596 Levchuk, S., Kashparov, V., Maloshtan, I., Yoschenko, V., Van Meir, N., 2012. Migration of
597 transuranic elements in groundwater from the near-surface radioactive waste site. Applied
598 Geochemistry, 27(7): 1339-1347.
599 Li, N., Ren, L., 2009. Application of continuous time random walk theory to nonequilibrium
600 transport in soil. Journal of contaminant hydrology, 108(3): 134-151.
601 Maderich, V. et al., 2014. Dispersion and fate of 90 Sr in the Northwestern Pacific and adjacent seas:
602 Global fallout and the Fukushima Dai-ichi accident. Science of The Total Environment, 494:
603 261-271.
604 Margolin, G., Dentz, M., Berkowitz, B., 2003. Continuous time random walk and multirate mass
605 transfer modeling of sorption. Chemical physics, 295(1): 71-80.

606 Miller, W.M., Chapman, N., McKinley, I., Alexander, R., Smellie, J., 1994. Natural analogue studies
607 in the geological disposal of radioactive wastes. Elsevier.
608 Neuman, S.P., Tartakovsky, D.M., 2009. Perspective on theories of non-Fickian transport in
609 heterogeneous media. Advances in Water Resources, 32(5): 670-680.
610 Qian, T., Li, S., Ding, Q., Wu, G., Zhao, D., 2009. Two-dimensional numerical modeling of 90 Sr
611 transport in an unsaturated Chinese loess under artificial sprinkling. Journal of environmental
612 radioactivity, 100(5): 422-428.
613 Rhodes, M.E., Bijeljic, B., Blunt, M.J., 2008. Pore-to-field simulation of single-phase transport using
614 continuous time random walks. Advances in water resources, 31(12): 1527-1539.
615 Rod, K.A., Um, W., Flury, M., 2010. Transport of strontium and cesium in simulated Hanford tank
616 waste leachate through quartz sand under saturated and unsaturated flow. Environmental
617 science & technology, 44(21): 8089-8094.
618 Rubin, S., Dror, I., Berkowitz, B., 2012. Experimental and modeling analysis of coupled non-Fickian
619 transport and sorption in natural soils. Journal of contaminant hydrology, 132: 28-36.
620 Rumynin, V.G., 2011. Subsurface Solute Transport Models and Case Histories: With Applications to
621 Radionuclide Migration, 25. Springer Science & Business Media.
622 Scher, H., Lax, M., 1973. Stochastic transport in a disordered solid. I. Theory. Physical Review B,
623 7(10): 4491.
624 Šimůnek, J., van Genuchten, M.T., 2008. Modeling nonequilibrium flow and transport processes
625 using HYDRUS. Vadose Zone Journal, 7(2): 782-797.
626 Šimůnek, J., van Genuchten, M.T., Šejna, M., 2008. Development and applications of the HYDRUS
627 and STANMOD software packages and related codes. Vadose Zone Journal, 7(2): 587-600.
628 Šimůnek, J., Van Genuchten, M.T., Šejna, M., Toride, N., Leij, F., 1999. The STANMOD computer
629 software for evaluating solute transport in porous media using analytical solutions of

convection–dispersion equation. Versions 1.0 and 2.0. International Ground Water Modeling Center.

Srinivasan, P., Sarmah, A.K., 2014. Assessing the sorption and leaching behaviour of three sulfonamides in pasture soils through batch and column studies. Science of The Total Environment, 493: 535-543.

Toride, N., Leij, F., Van Genuchten, M.T., 1995. The CXTFIT code for estimating transport parameters from laboratory and field tracer experiments.

Volkova, E., 2009. Sensitivity analysis of the numerical simulation of 90Sr transport for old repositories at the Russian Science Center Kurchatov Institute. Atomic energy, 106(4): 287-293.

Wang, L., Cardenas, M.B., 2014. Non-Fickian transport through two-dimensional rough fractures: Assessment and prediction. Water Resources Research, 50(2): 871-884.

Yin, J., Jeen, S.-W., Lee, D.R., Mayer, K.U., 2014. Reactive transport modeling of 90 Sr sorption in reactive sandpacks. Journal of hazardous materials, 280: 685-695.

646 **Tables**

647 **Table 1** Relationship between β and transport regimes[1]

Value	Characteristics of parameters	Transport feature
$0<\beta<1$	The first and the second moment of the $\psi(t)$ is inexistence; both transport velocity and dispersion coefficient vary with time as power laws.	Indicates a highly non-Fickian dispersion transport.
$1<\beta<2$	The second moment of the $\psi(t)$ does not exist, where transport velocity is constant but dispersion coefficient still vary with time.	Presents moderate non-Fickian transport or moderately dispersive systems.
$\beta \geqslant 2$	The first and second moments of the $\psi(t)$ exist, both transport velocity and dispersion coefficient are constant.	Displays Fickian transport, Gaussian distributions of plume

648 [1] Summarized from Li and Ren (2009), Wang and Cardenas (2014).

649

650

651 **Table 2** Fitted values of parameters for ADE and CTRW

	ADE (CXTFIT)			CTRW (MATLAB toolbox)						
	v^1 (cm/d)	D^1 (cm^2/d)	R^1	v_ψ (cm/d)	D_ψ (cm^2/d)	β	t_1(d)	t_2 (d)	Λ	μ
a	79.78±5.78	286.56±1.44	0.997±0.111	55.34	178.56	1.80	1.48E-2	1.09	0.05	0.01
b	46.30±3.22	67.25±15.50	1.017±0.069	11.23	30.65	2.16	4.32E-2	5.93	0.04	0.01
c	22.50±0.59	11.10±2.20	1.039±0.027	10.8	3.44	2.27	4.25E-2	4.60	0.03	0.03
d	9.21±9.20	22.37 ±4.79	0.999±0.111	20.25	215.94	0.31	2.05E-2	4.06E3	0.09	0.08
e	1.05±0.01	0.57 ±0.03	1.053±0.027	0.52	0.12	1.43	2.53 E-1	3.62E3	0.12	0.12

f	0.83±0.01	0.55±0.04	1.076±0.048	0.47	0.10	1.26	3.69 E-1	6.59E3	0.13	0.09
g	0.67±0.01	0.47±0.04	1.093±0.029	0.38	0.12	0.62	6.24E-1	6.89E3	0.15	0.15
h	0.58±0.01	0.43±0.06	1.194±0.017	0.31	0.03	0.87	9.11E-1	1.07E4	0.18	0.16

652 Columns a-d: packed by sand, with sprinkling volumetric flow rate Q =100, 50, 20, 2 mL/d,
653 respectively; Columns e-h: Q=2 mL/d, packed by sand+clay (3:1), sand+clay (1:1), sand+clay (1:3) ,
654 clay, respectively.
655 [1]: The parameters values with 95% confidence limits.
656
657
658 **Table 3** Estimated values of Peclet number for the columns

column	a	b	c	d	e	f	g	h
Pe[1]	4.6~5.6	9.4~17.2	29.6~56.1	0.01~18.8	31.2~78	25.1~84.6	23.3~57	20.9~186

659 [1]: The values were estimated using the inverse modelling results listed in Table 2.
660

661 **Figure captions**

662

663 **Fig. 1.** Schematic illustration of the experimental setup

664

665 **Fig. 2.** Simulated leach concentrations of bromine (a) and strontium (b) over column experimental
666 duration under different sprinkling volumetric flow rate (*Q)* conditions according to equations (2~3).

667

668 **Fig. 3.** Observed cumulative mass fraction of bromine (a) and strontium (b) eluted from
669 corresponding columns, calculated by Equation (13). Columns a-d: packed by sand, sprinkling
670 volume flow rate Q =100, 50, 20, 2 mL/d, respectively; Columns e-h: Q=2 mL/d, packed by sand
671 and clay (3:1), sand and clay (1:1), sand and clay (1:3), clay, respectively.

672

673 **Fig. 4.** Measured and best fitted BTCs of strontium using ADE/CTRW for column experiments. The
674 corresponding fitted values of parameters for the columns are shown in Table 2. The first four
675 columns (a-d) are packed with sand, with sprinkling volume flow rate Q =100, 50, 20, 2 mL/d,
676 respectively; the next three columns (e-h) are packed with different ratios of sand to clay: e 3:1, f 1:1,
677 g 1:3, respectively. The column-h was packed with clay. Note that columns e-h are used by applying
678 the same volumetric flow rate 2 mL/d. Dashed line is the equilibrium ADE model fit and solid line is
679 the CTRW-based TPL model fit.

680

681

Fig. 1

Click here to download high resolution image

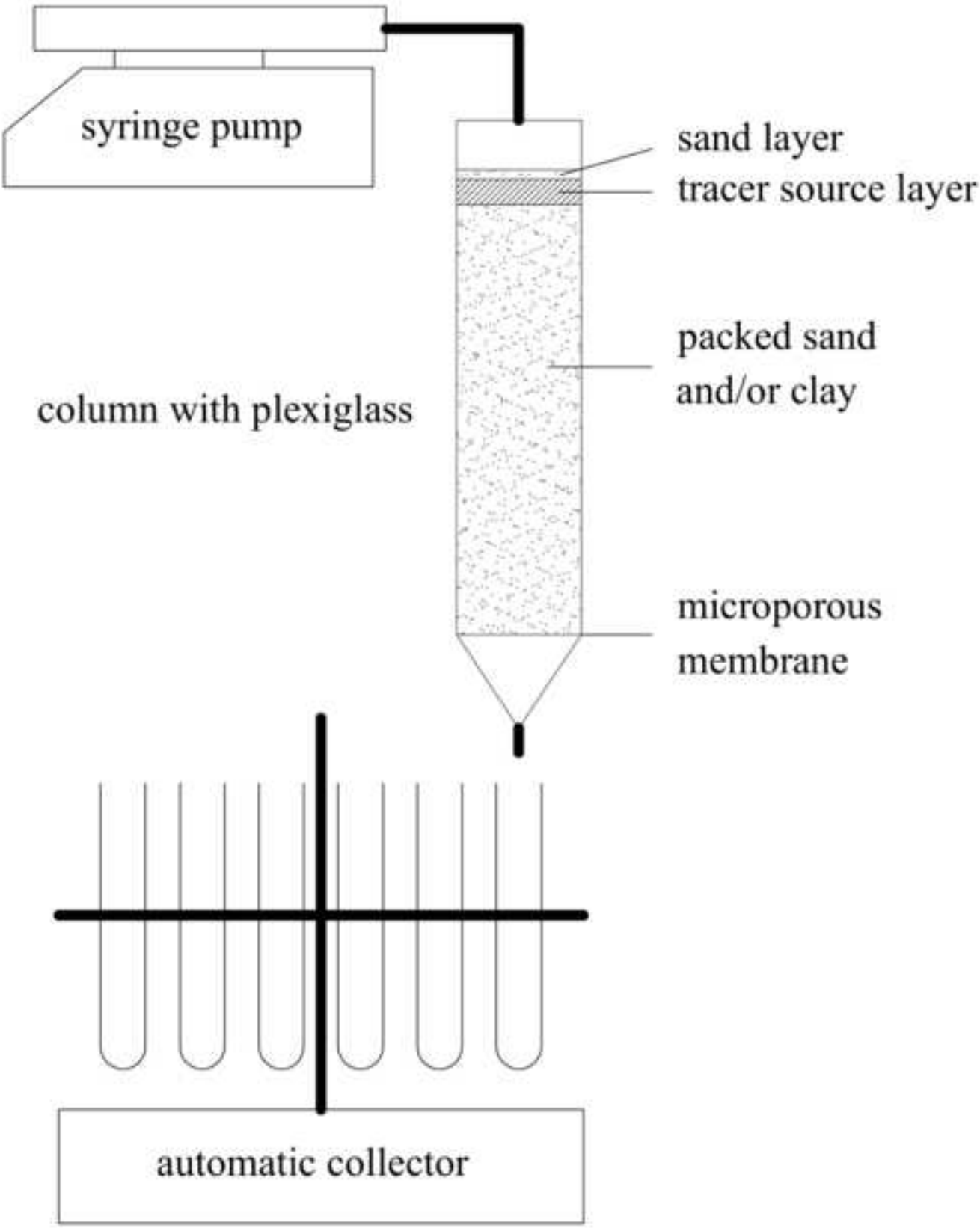

Fig. 2a

Click here to download high resolution image

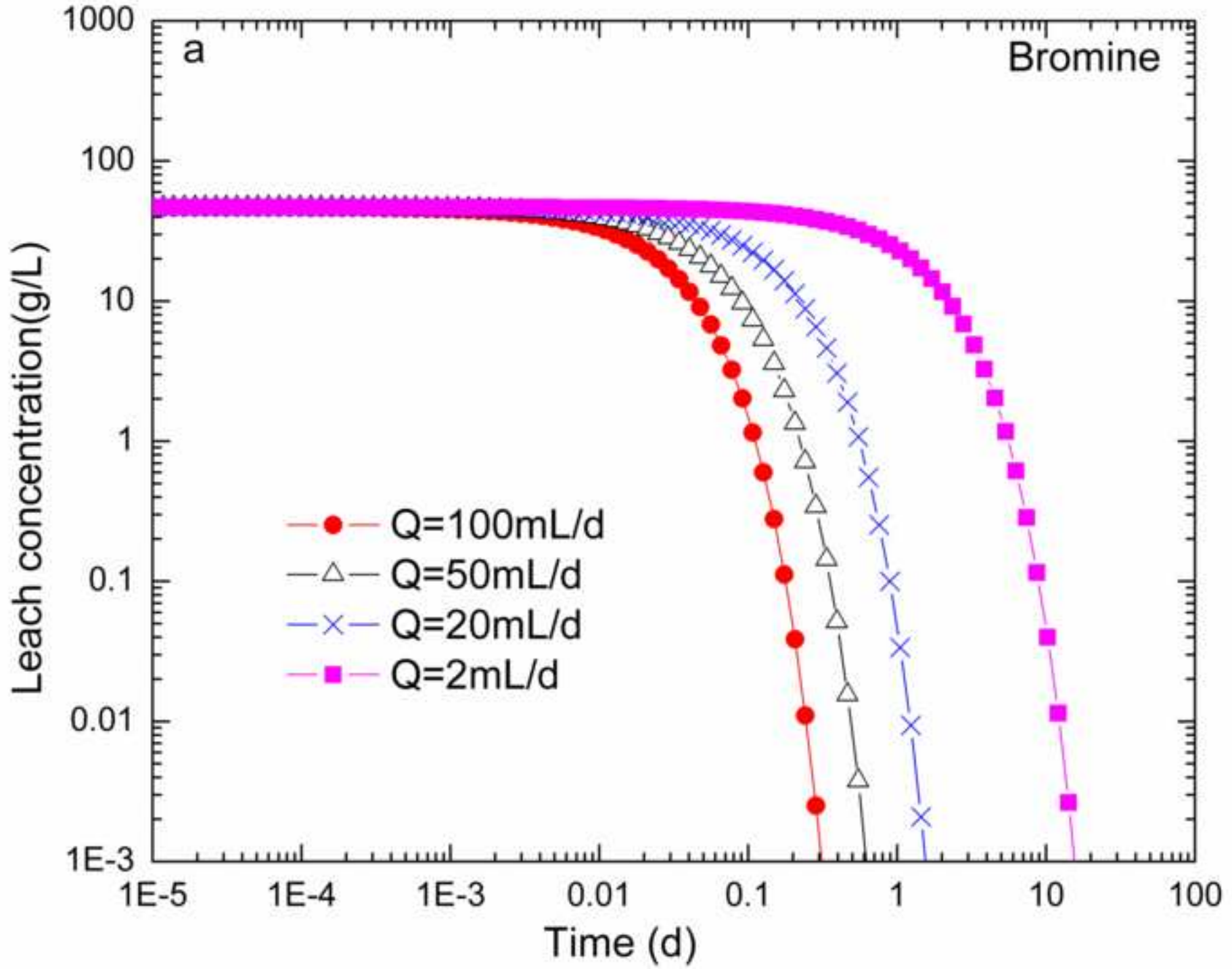

Fig. 2b

Click here to download high resolution image

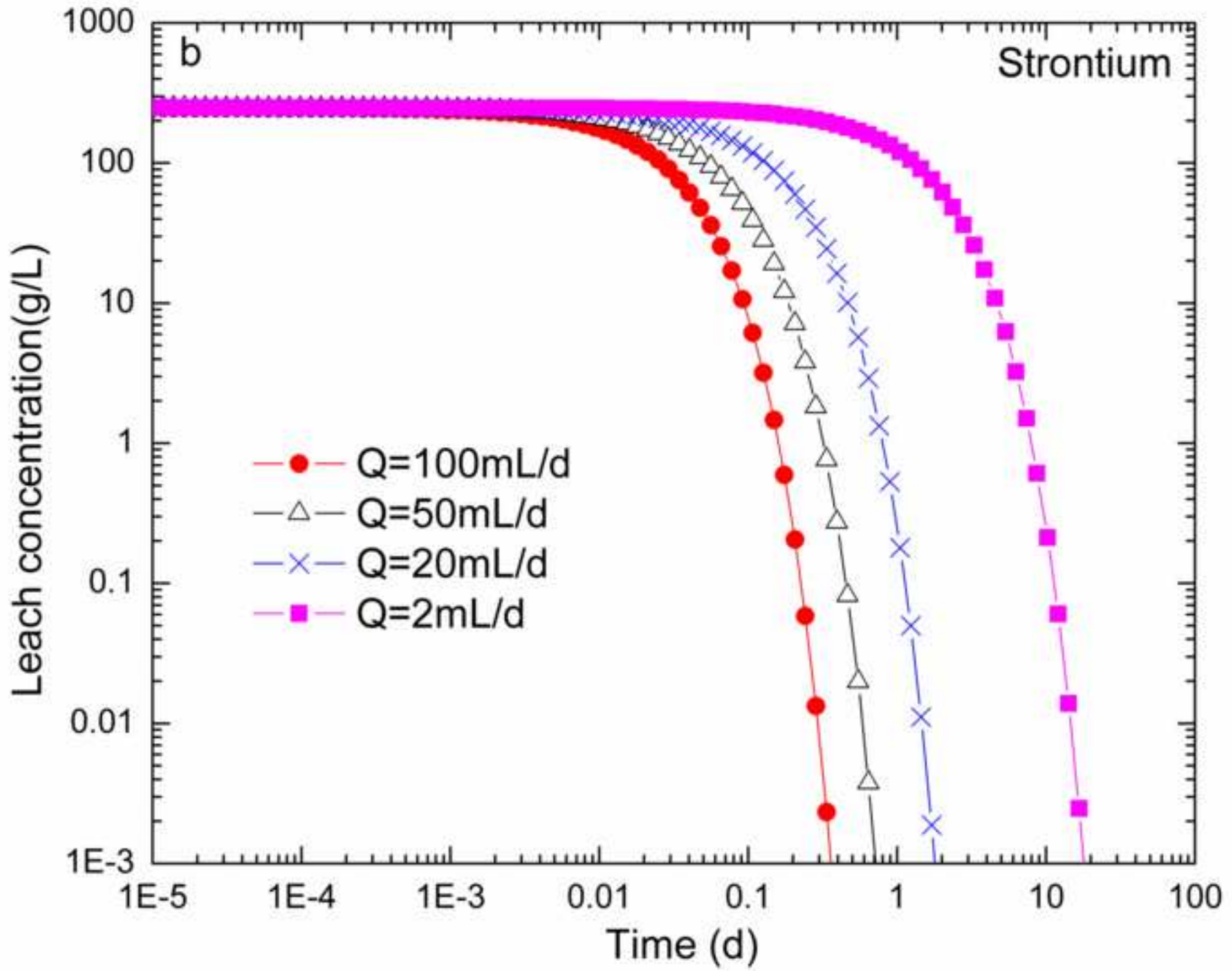

Fig. 3a

Click here to download high resolution image

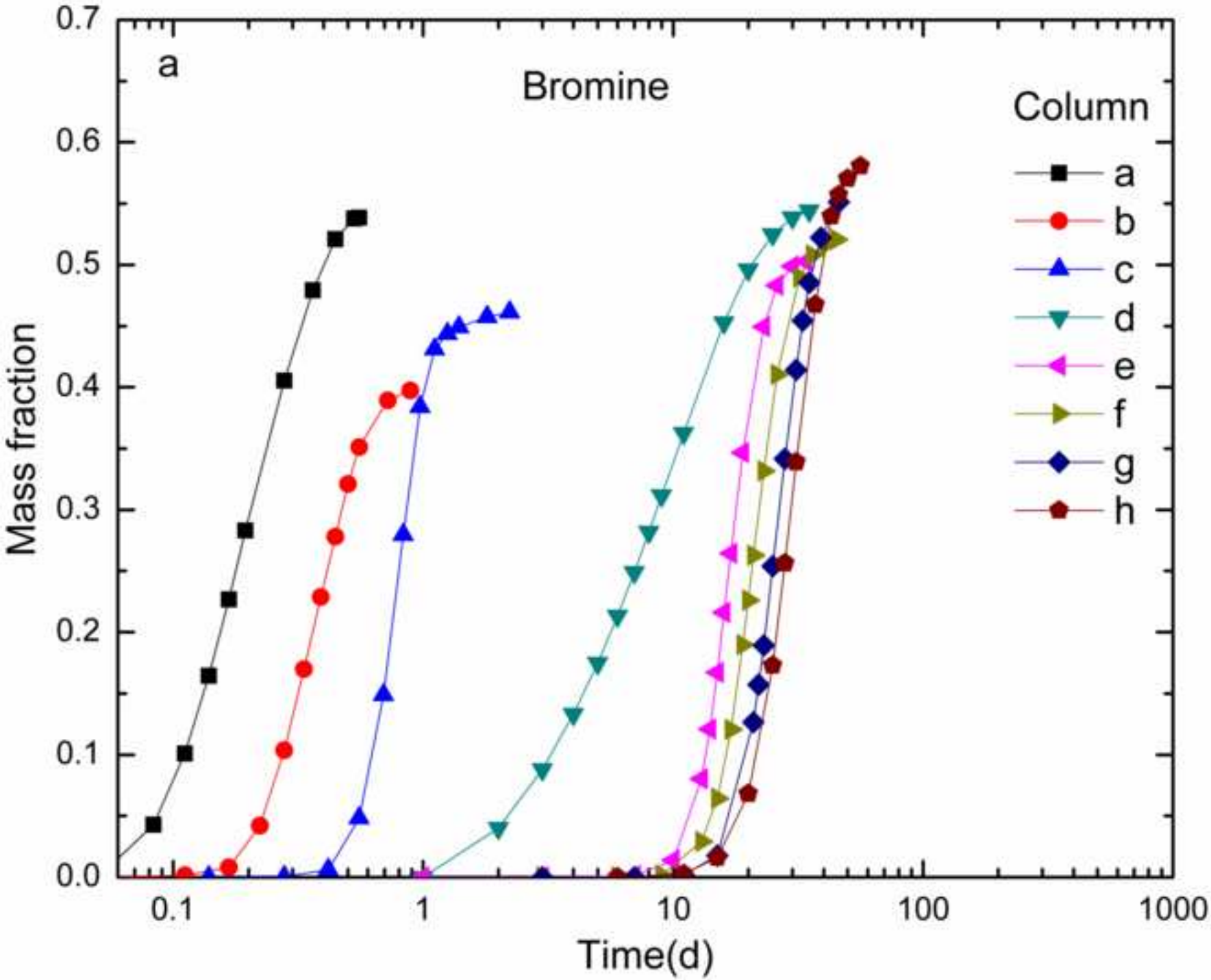

Fig. 3b

Click here to download high resolution image

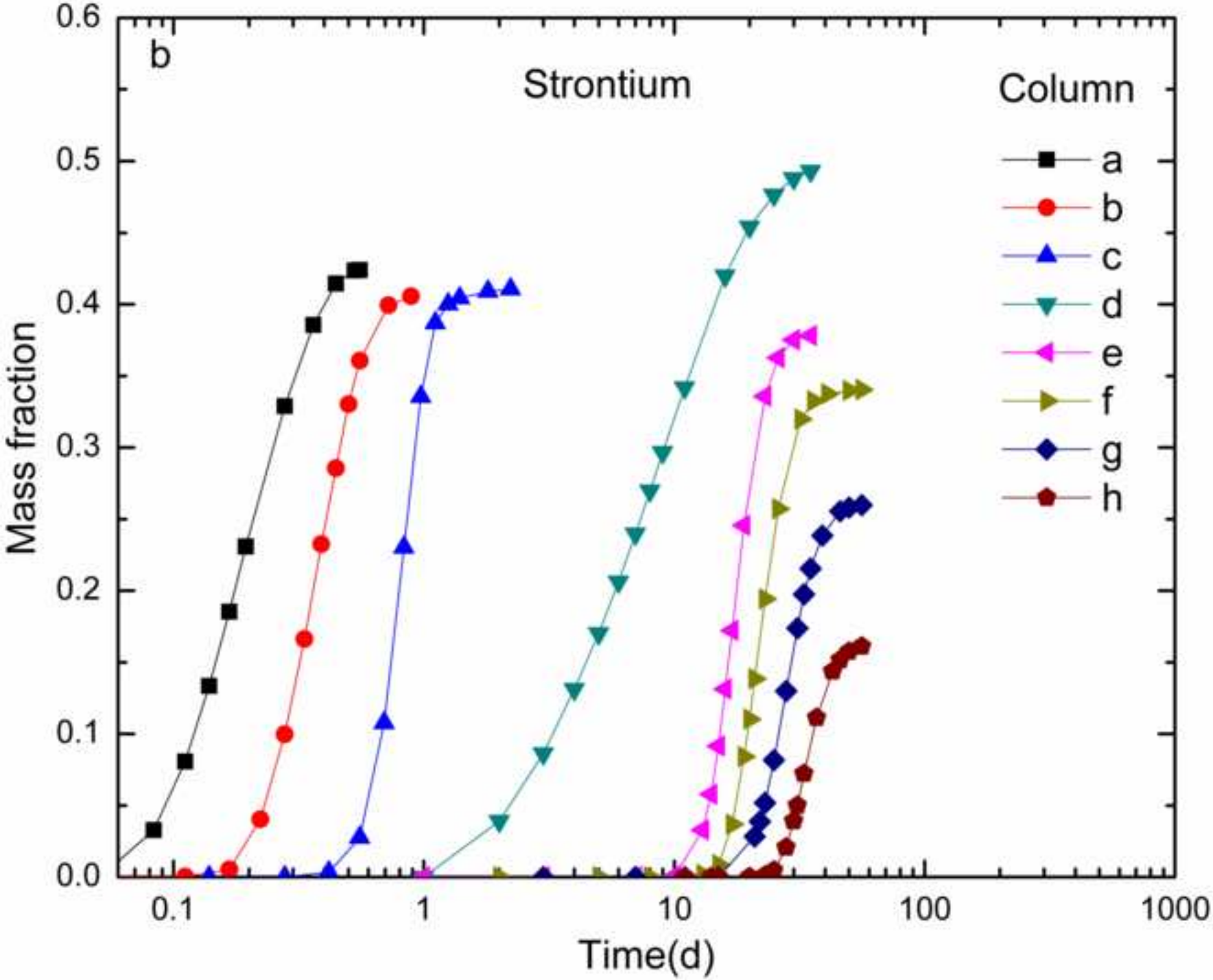

Fig. 4a

Click here to download high resolution image

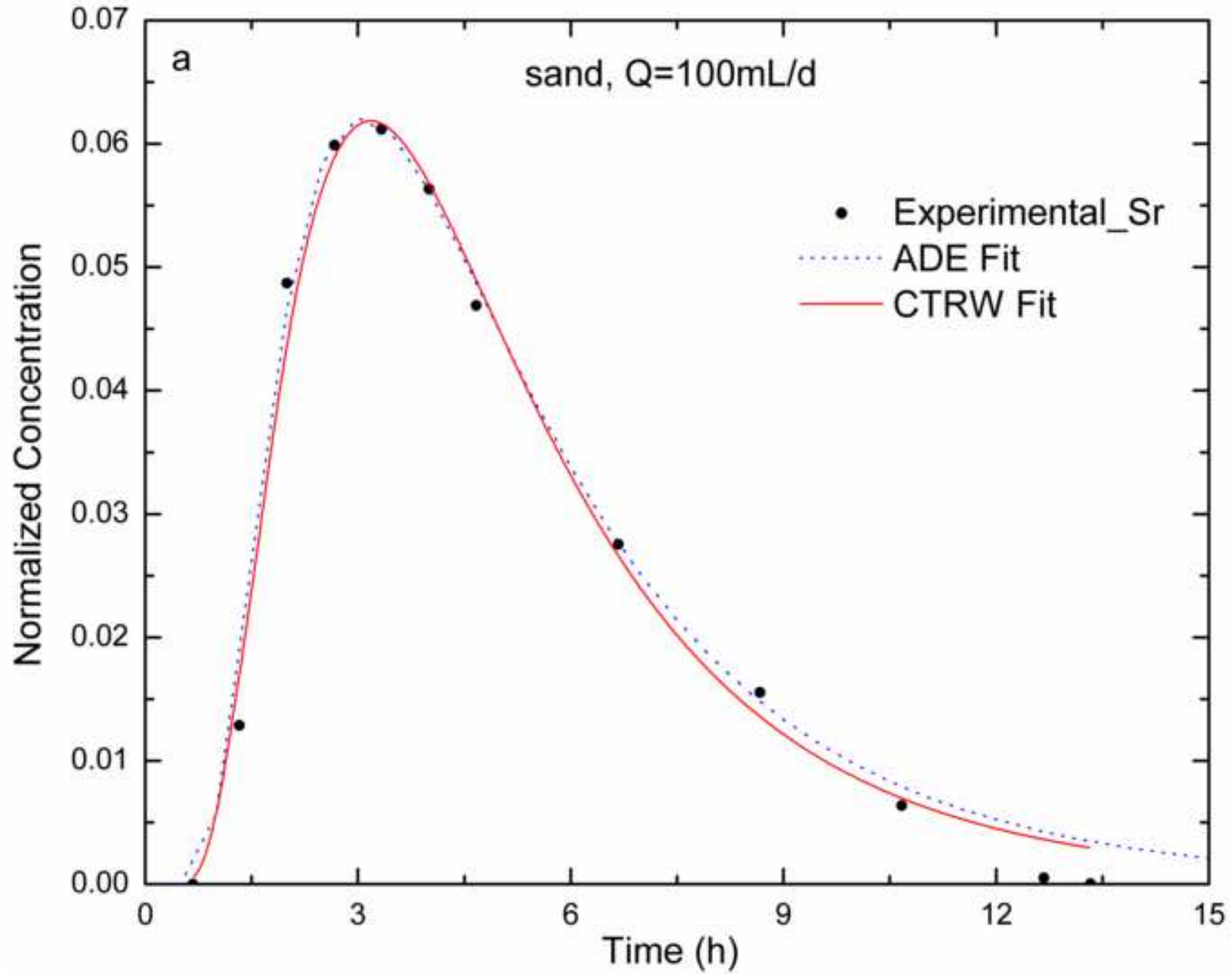

Fig. 4b

Click here to download high resolution image

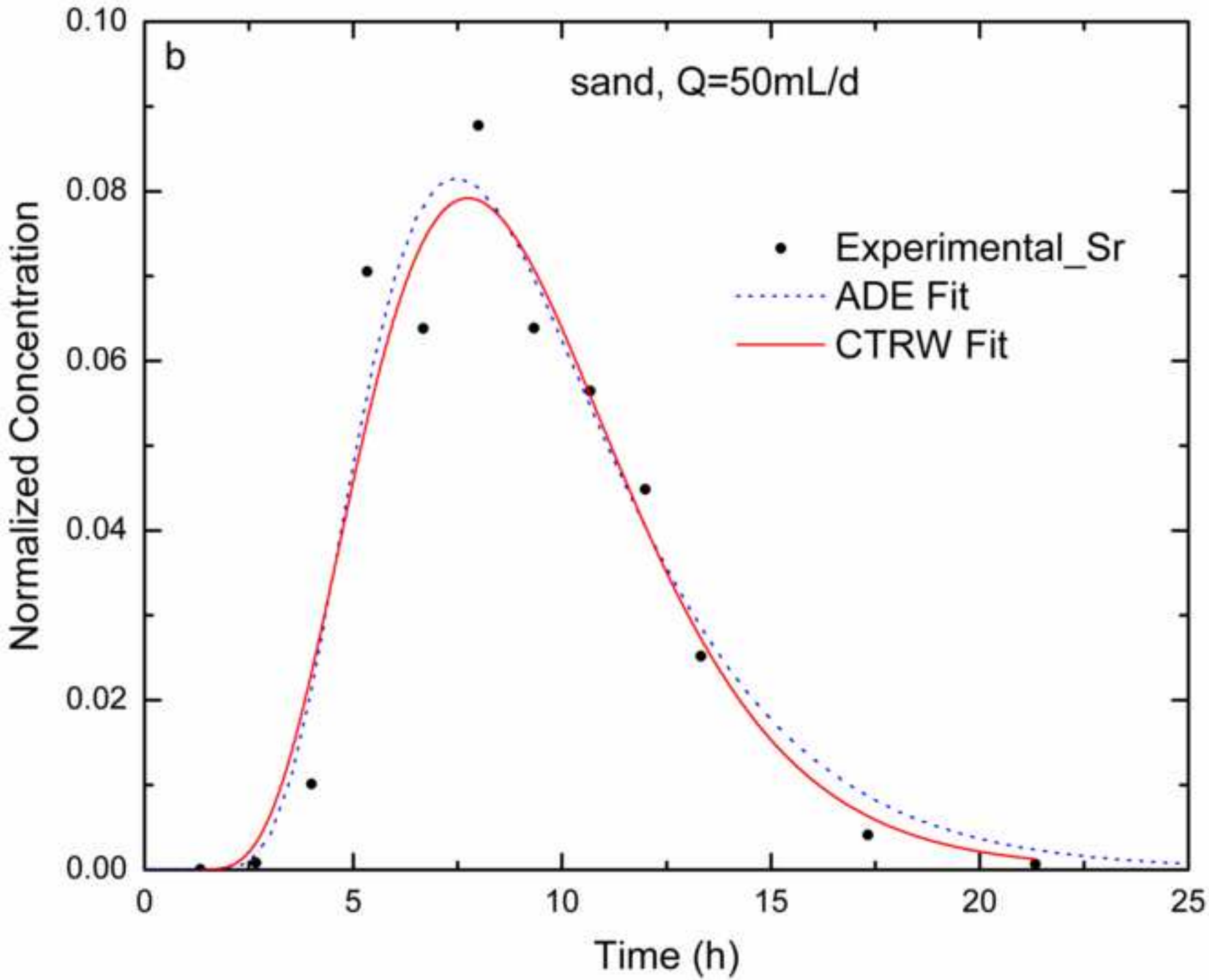

Fig. 4c

Click here to download high resolution image

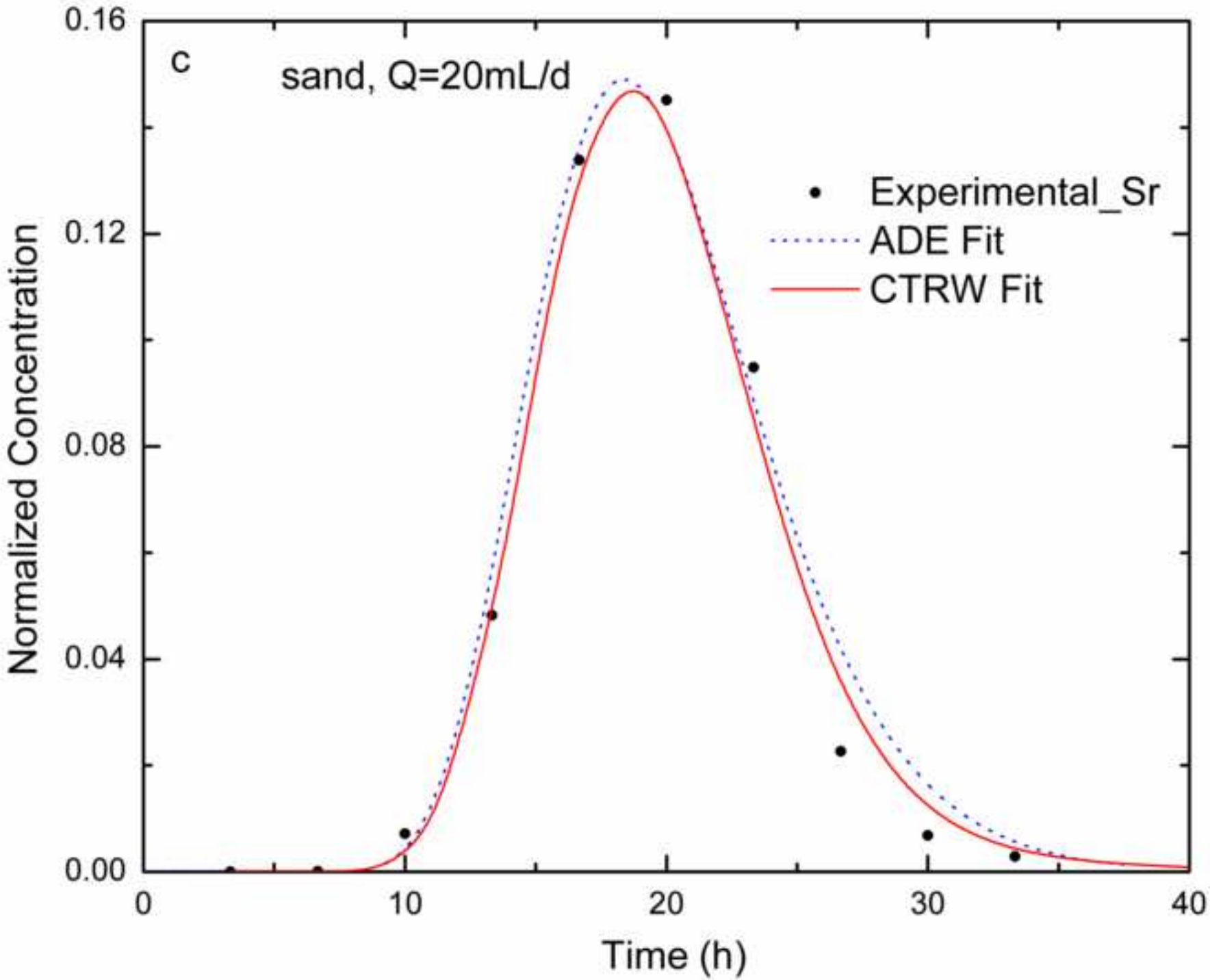

Fig. 4d

Click here to download high resolution image

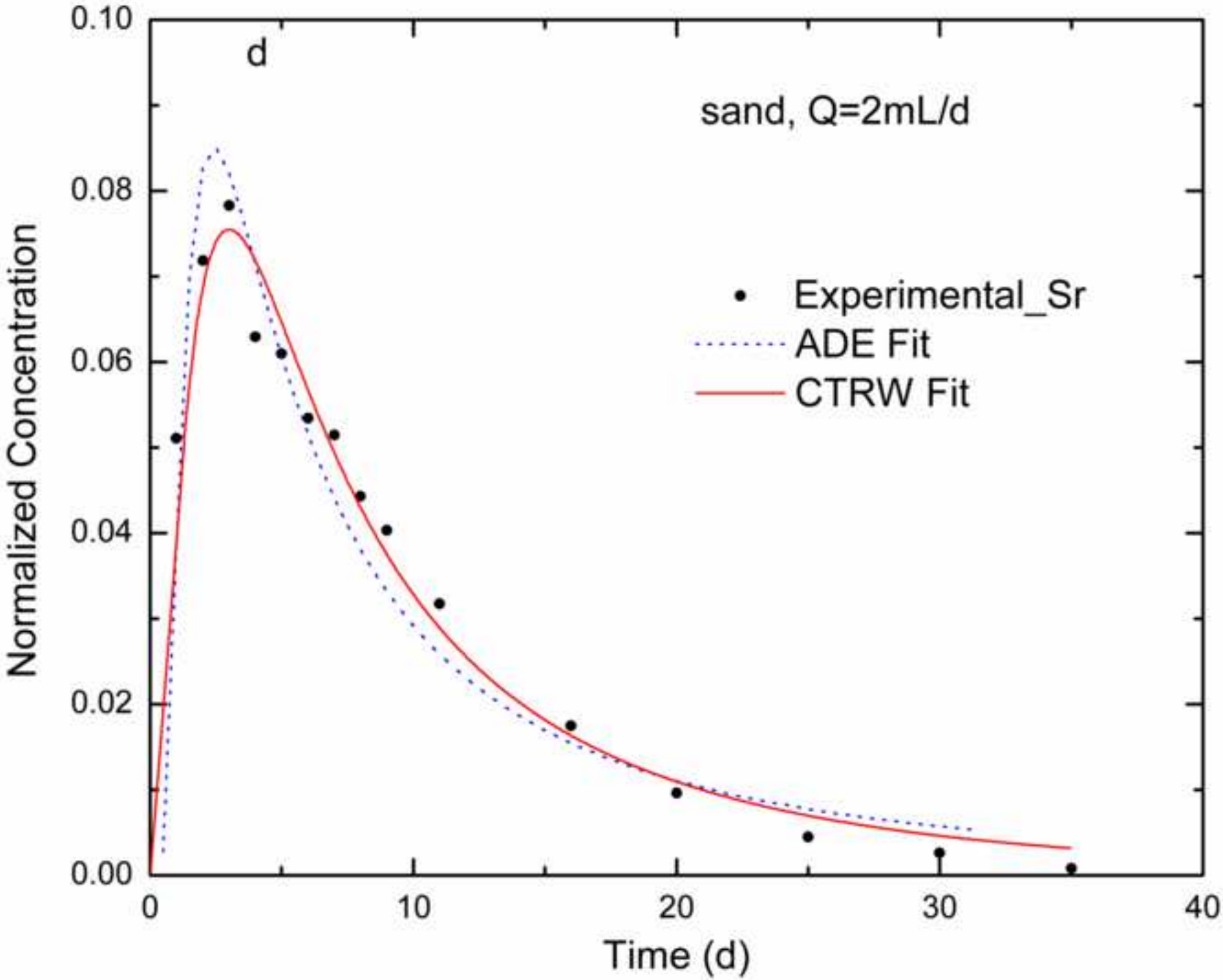

Fig. 4e

Click here to download high resolution image

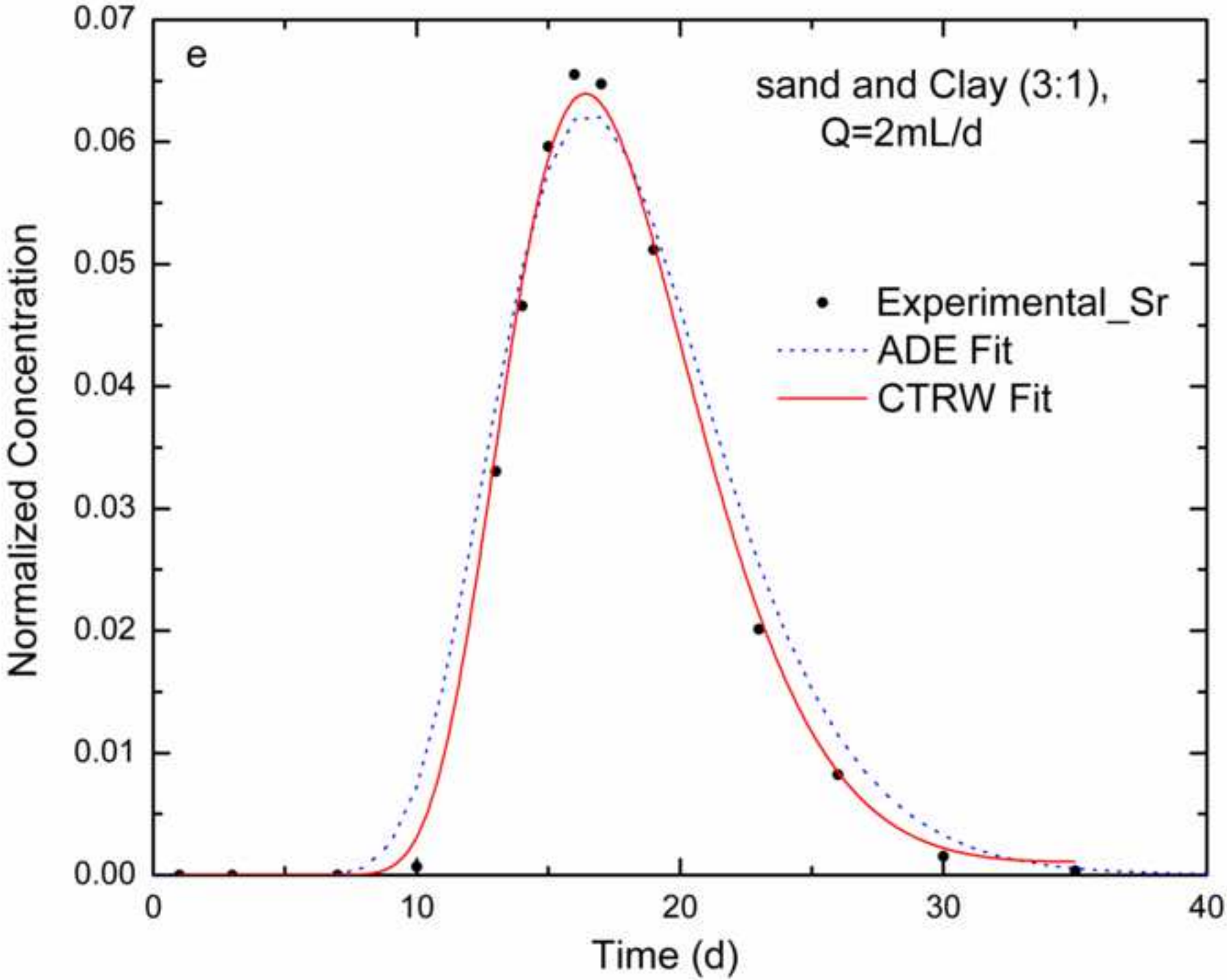

Fig. 4f

Click here to download high resolution image

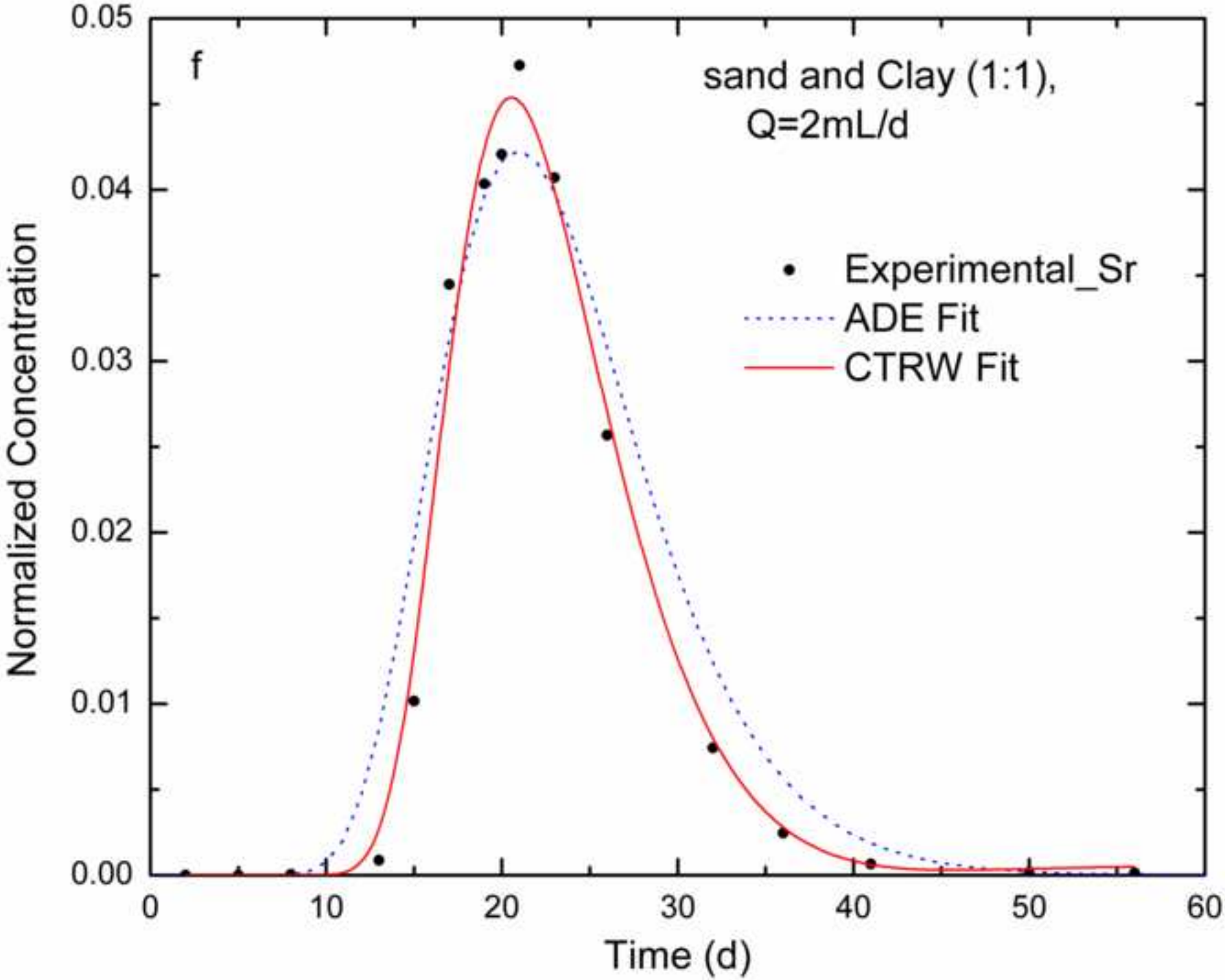

Fig. 4g

Click here to download high resolution image

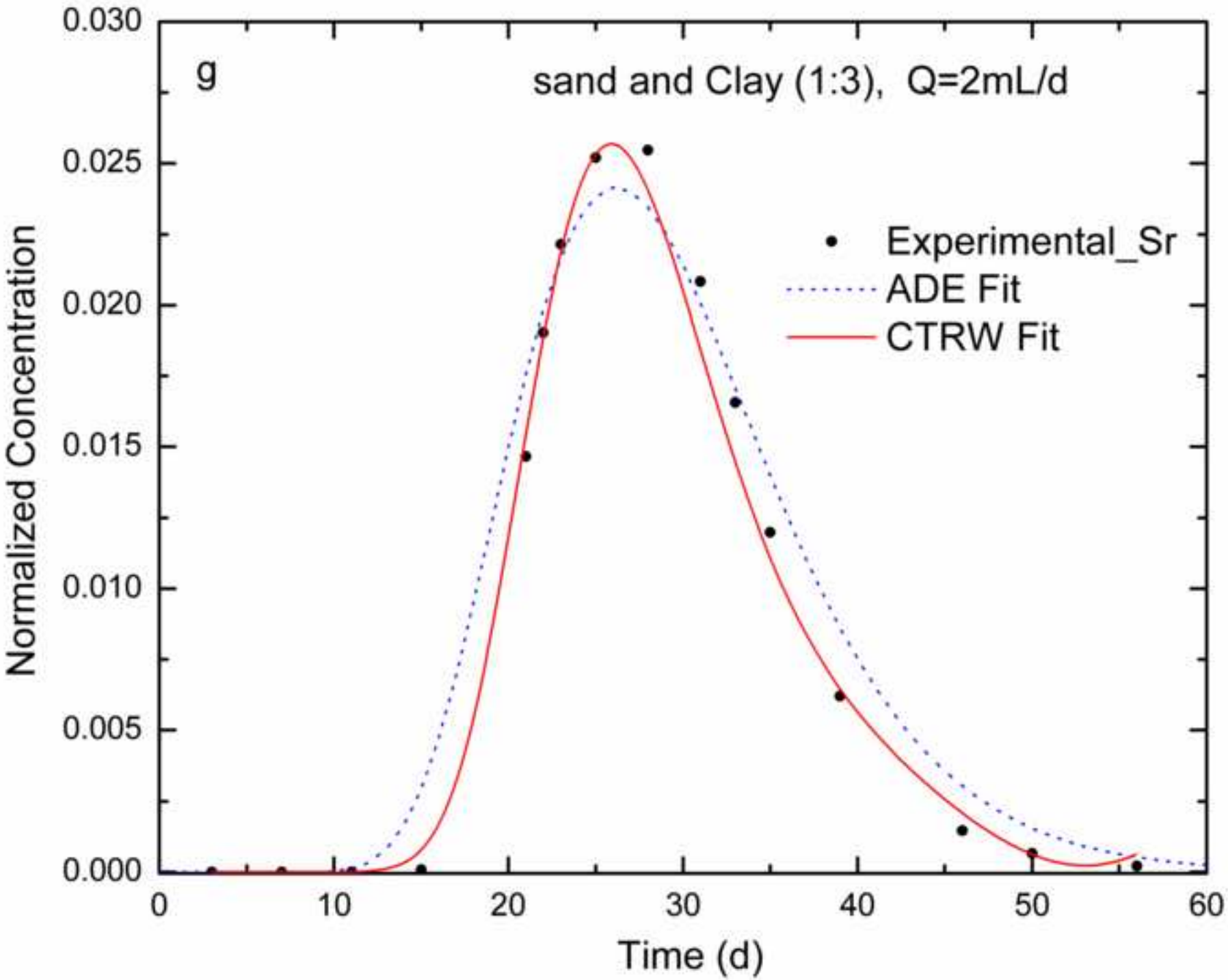

Fig. 4h

Click here to download high resolution image

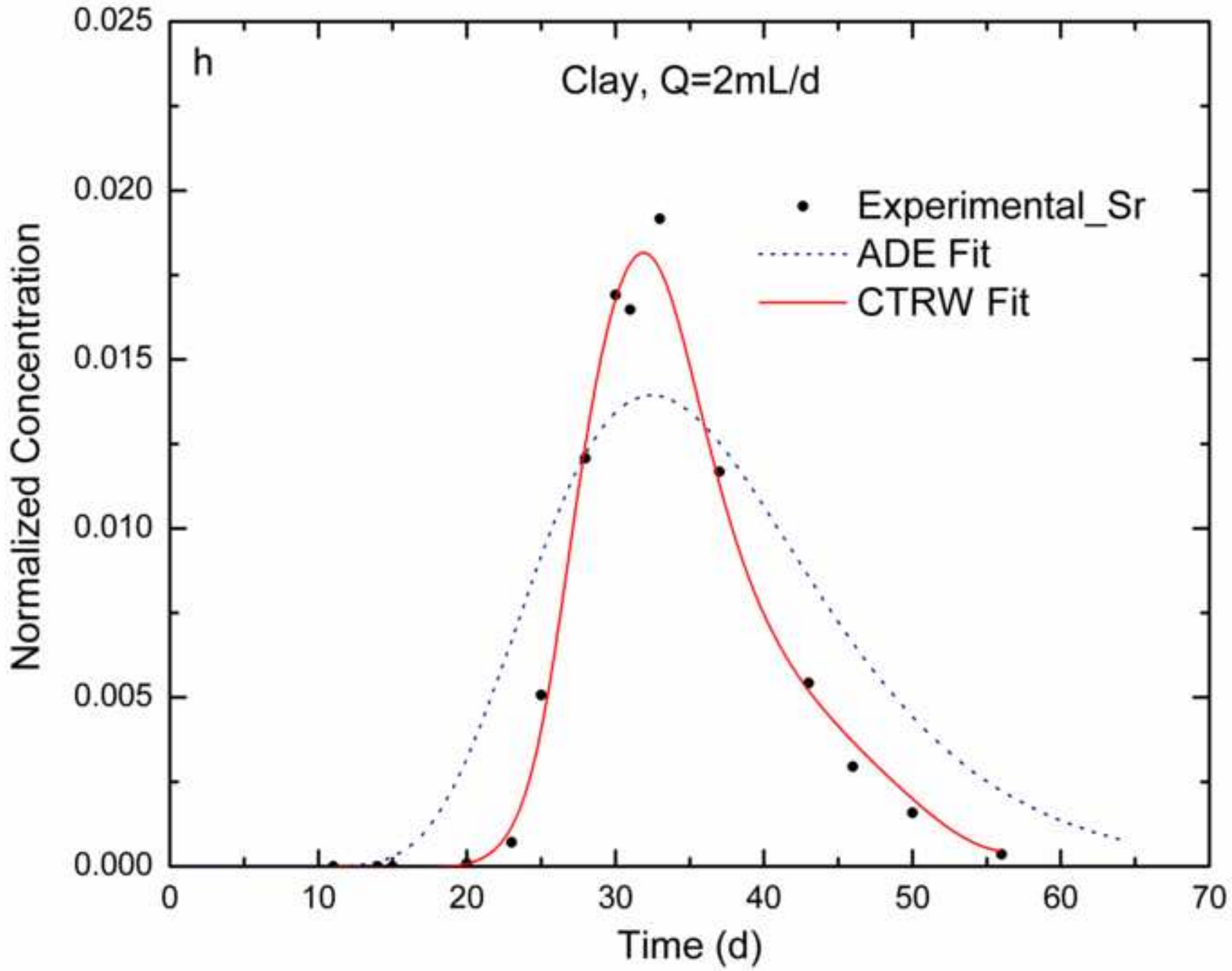

Table 1 Relationship between β and transport regimes[1]

Value	Characteristics of parameters	Transport feature
$0<\beta<1$	The first and the second moment of the $\psi(t)$ is inexistence; both transport velocity and dispersion coefficient vary with time as power laws.	Indicates a highly non-Fickian dispersion transport.
$1<\beta<2$	The second moment of the $\psi(t)$ does not exist, where transport velocity is constant but dispersion coefficient still vary with time.	Presents moderate non-Fickian transport or moderately dispersive systems.
$\beta\geqslant 2$	The first and second moments of the $\psi(t)$ exist, both transport velocity and dispersion coefficient are constant.	Displays Fickian transport, Gaussian distributions of plume

[1] Summarized from Li and Ren (2009), Wang and Cardenas (2014).

Table 2 Fitted values of parameters for ADE and CTRW

	ADE (CXTFIT)			CTRW (MATLAB toolbox)						
	v^1 (cm/d)	D^1 (cm^2/d)	R^1	v_ψ (cm/d)	D_ψ (cm^2/d)	β	t_1(d)	t_2 (d)	Λ	μ
a	79.78±5.78	286.56±1.44	0.997±0.111	55.34	178.56	1.80	1.48E-2	1.09	0.05	0.01
b	46.30±3.22	67.25±15.50	1.017±0.069	11.23	30.65	2.16	4.32E-2	5.93	0.04	0.01
c	22.50±0.59	11.10±2.20	1.039±0.027	10.8	3.44	2.27	4.25E-2	4.60	0.03	0.03
d	9.21±9.20	22.37 ±4.79	0.999±0.111	20.25	215.94	0.31	2.05E-2	4.06E3	0.09	0.08
e	1.05±0.01	0.57 ±0.03	1.053±0.027	0.52	0.12	1.43	2.53 E-1	3.62E3	0.12	0.12
f	0.83±0.01	0.55±0.04	1.076±0.048	0.47	0.10	1.26	3.69 E-1	6.59E3	0.13	0.09
g	0.67±0.01	0.47±0.04	1.093±0.029	0.38	0.12	0.62	6.24E-1	6.89E3	0.15	0.15
h	0.58±0.01	0.43±0.06	1.194±0.017	0.31	0.03	0.87	9.11E-1	1.07E4	0.18	0.16

Columns a-d: packed by sand, with sprinkling volumetric flow rate Q =100, 50, 20, 2 mL/d, respectively; Columns e-h: Q=2 mL/d, packed by sand+clay (3:1), sand+clay (1:1), sand+clay (1:3) , clay, respectively.

[1]: The parameters values with 95% confidence limits.

Table 3 Estimated values of Peclet number for the columns

column	a	b	c	d	e	f	g	h
Pe[1]	4.6~5.6	9.4~17.2	29.6~56.1	0.01~18.8	31.2~78	25.1~84.6	23.3~57	20.9~186

[1]: The values were estimated using the inverse modelling results listed in Table 2.